



# Standard Test Method for Determining Residual Stresses by the Hole-Drilling Strain- Gage Method<sup>1</sup>

This standard is issued under the fixed designation E 837; the number immediately following the designation indicates the year of original adoption or, in the case of revision, the year of last revision. A number in parentheses indicates the year of last reapproval. A superscript epsilon (ε) indicates an editorial change since the last revision or reapproval.

## INTRODUCTION

The hole-drilling strain-gage method determines residual stresses near the surface of an isotropic linear-elastic material. It involves attaching a strain rosette to the surface, drilling a hole at the geometric center of the rosette, and measuring the resulting relieved strains. The residual stresses within the removed material are then determined from the measured strains using a series of equations.

## 1. Scope

### 1.1 Residual Stress Determination:

1.1.1 This test method specifies a hole-drilling procedure for determining residual stress profiles near the surface of an isotropic linearly elastic material. The test method is applicable to residual stress profile determinations where in-plane stress gradients are small. The stresses may remain approximately constant with depth (“uniform” stresses) or they may vary significantly with depth (“non-uniform” stresses). The measured workpiece may be “thin” with thickness much less than the diameter of the drilled hole or “thick” with thickness much greater than the diameter of the drilled hole. Only uniform stress measurements are specified for thin workpieces, while both uniform and non-uniform stress measurements are specified for thick workpieces.

### 1.2 Stress Measurement Range:

1.2.1 The hole-drilling method can identify in-plane residual stresses near the measured surface of the workpiece material. The method gives localized measurements that indicate the residual stresses within the boundaries of the drilled hole.

1.2.2 This test method applies in cases where material behavior is linear-elastic. In theory, it is possible for local yielding to occur due to the stress concentration around the drilled hole, for isotropic (equi-biaxial) residual stresses exceeding 50 % of the yield stress, or for shear stresses in any direction exceeding 25 % of the yield stress. However, in practice it is found that satisfactory results can be achieved providing the residual stresses do not exceed about 60 % of the material yield stress.

### 1.3 Workpiece Damage:

1.3.1 The hole-drilling method is often described as “semi-destructive” because the damage that it causes is localized and often does not significantly affect the usefulness of the workpiece. In contrast, most other mechanical methods for measuring residual stresses substantially destroy the workpiece. Since hole drilling does cause some damage, this test method should be applied only in those cases either where the workpiece is expendable, or where the introduction of a small shallow hole will not significantly affect the usefulness of the workpiece.

1.4 *This standard does not purport to address all of the safety concerns, if any, associated with its use. It is the responsibility of the user of this standard to establish appropriate safety and health practices and determine the applicability of regulatory limitations prior to use.*

## 2. Referenced Documents

### 2.1 ASTM Standards:<sup>2</sup>

**E 251** Test Methods for Performance Characteristics of Metallic Bonded Resistance Strain Gages

## 3. Terminology

### 3.1 Symbols:

$\bar{a}$	= calibration constant for isotropic stresses
$\bar{b}$	= calibration constant for shear stresses
$\bar{a}_{jk}$	= calibration matrix for isotropic stresses
$\bar{b}_{jk}$	= calibration matrix for shear stresses
$D$	= diameter of the gage circle, see Table 1.

<sup>1</sup> This test method is under the jurisdiction of ASTM Committee E28 on Mechanical Testing and is the direct responsibility of Subcommittee E28.13 on Residual Stress Measurement.

Current edition approved Feb. 1, 2008. Published April 2008. Originally approved in 1981. Last previous edition approved in 2001 as E 837 – 01 <sup>ε1</sup>.

<sup>2</sup> For referenced ASTM standards, visit the ASTM website, [www.astm.org](http://www.astm.org), or contact ASTM Customer Service at [service@astm.org](mailto:service@astm.org). For *Annual Book of ASTM Standards* volume information, refer to the standard's Document Summary page on the ASTM website.

$D_0$	= diameter of the drilled hole
$E$	= Young's modulus
$j$	= number of hole depth steps so far
$k$	= sequence number for hole depth steps
$P$	= uniform isotropic (equi-biaxial) stress
$P_k$	= isotropic stress within hole depth step $k$
$p$	= uniform isotropic (equi-biaxial) strain
$p_k$	= isotropic strain after hole depth step $k$
$Q$	= uniform 45° shear stress
$Q_k$	= 45° shear stress within hole depth step $k$
$q$	= uniform 45° shear strain
$q_k$	= 45° shear strain after hole depth step $k$
$T$	= uniform x-y shear stress
$T_k$	= x-y shear stress within hole depth step $k$
$t$	= x-y shear strain
$t_k$	= x-y shear strain after hole depth step $k$
$T$	= (superscript) matrix transpose
$\alpha_P$	= regularization factor for $\mathbf{P}$ stresses
$\alpha_Q$	= regularization factor for $\mathbf{Q}$ stresses
$\alpha_T$	= regularization factor for $\mathbf{T}$ stresses
$\beta$	= clockwise angle from the x-axis (gage 1) to the maximum principal stress direction
$\epsilon$	= relieved strain for “uniform” stress case
$\epsilon_j$	= relieved strain measured after $j$ hole depth steps have been drilled
$\nu$	= Poisson's ratio
$\theta$	= angle of strain gage from the x-axis
$\sigma_{max}$	= maximum (more tensile) principal stress
$\alpha_{min}$	= minimum (more compressive) principal stress
$\sigma_x$	= uniform normal x-stress
$(\sigma_x)_k$	= normal x-stress within hole depth step $k$
$\sigma_y$	= uniform normal y-stress
$(\sigma_y)_k$	= normal y-stress within hole depth step $k$
$\tau_{xy}$	= uniform shear xy-stress
$(\tau_{xy})_k$	= shear xy-stress within hole depth step $k$

#### 4. Summary of Test Method

##### 4.1 Workpiece:

4.1.1 A flat uniform surface area away from edges and other irregularities is chosen as the test location within the workpiece of interest. Fig. 1 schematically shows the residual stresses acting at the test location at which a hole is to be drilled. These stresses are assumed to be uniform within the in-plane directions  $x$  and  $y$ .

NOTE 1—For reasons of pictorial clarity in Fig. 1, the residual stresses are shown as uniformly acting over the entire in-plane region around the test location. In actuality, it is not necessary for the residual stresses to be uniform over such a large region. The surface strains that will be relieved by drilling a hole depend only on the stresses that originally existed at the boundaries of the hole. The stresses beyond the hole boundary do not affect the relieved strains, even though the strains are measured beyond the hole boundary. Because of this, the hole-drilling method provides a very localized measurement of residual stresses.

4.1.2 Fig. 1(a) shows the case where the residual stresses in the workpiece are uniform in the depth direction. The in-plane stresses are  $\sigma_x$ ,  $\sigma_y$  and  $\tau_{xy}$  throughout the thickness. Uniform residual stress measurements can be made using this test method with “thin” workpieces whose material thickness is small compared with the hole and strain gage circle diameters, and with “thick” workpieces whose material thickness is large compared with the hole and strain gage circle diameters.

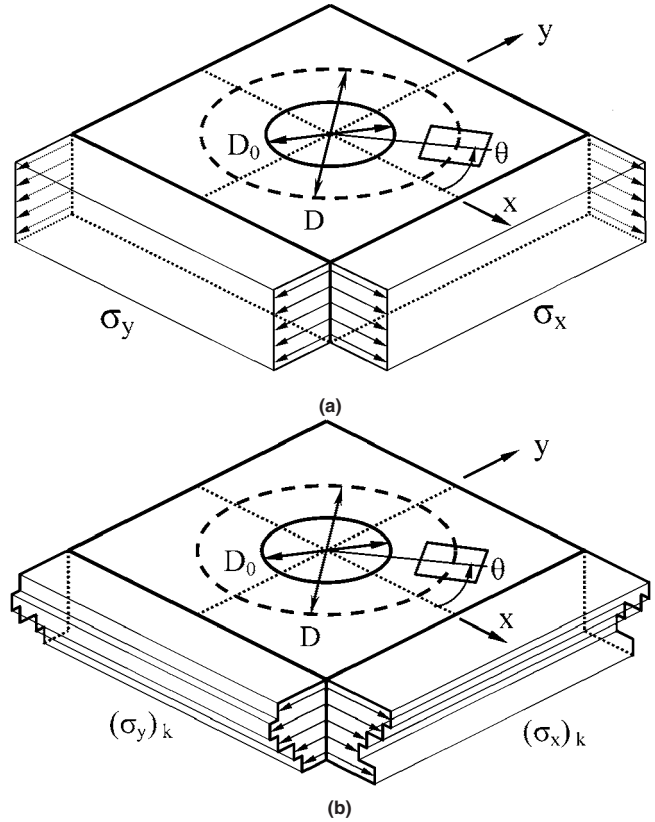


FIG. 1 Hole Geometry and Residual Stresses, (a) Uniform Stresses, (b) Non-uniform Stresses

4.1.3 Fig. 1(b) shows the case where the residual stresses in the workpiece vary in the depth direction. The calculation method described in this test method represents the stress profile as a staircase shape, where the depth steps correspond to the depth increments used during the hole-drilling measurements. Within depth step  $k$ , the in-plane stresses are  $(\sigma_x)_k$ ,  $(\sigma_y)_k$  and  $(\tau_{xy})_k$ . Non-uniform residual stress measurements can be made using this test method only with “thick” workpieces whose material thickness is large compared with the hole and strain gage circle diameters.

##### 4.2 Strain Gage Rosette::

4.2.1 A strain gage rosette with three or more elements of the general type schematically illustrated in Fig. 2 is attached to the workpiece at the location under consideration.

##### 4.3 Hole-Drilling:

4.3.1 A hole is drilled in a series of steps at the geometric center of the strain gage rosette.

4.3.2 The residual stresses in the material surrounding the drilled hole are partially relieved as the hole is drilled. The associated relieved strains are measured at a specified sequence of steps of hole depth using a suitable strain-recording instrument.

##### 4.4 Residual Stress Calculation Method:

4.4.1 The residual stresses originally existing at the hole location are evaluated from the strains relieved by hole-drilling using mathematical relations based on linear elasticity theory

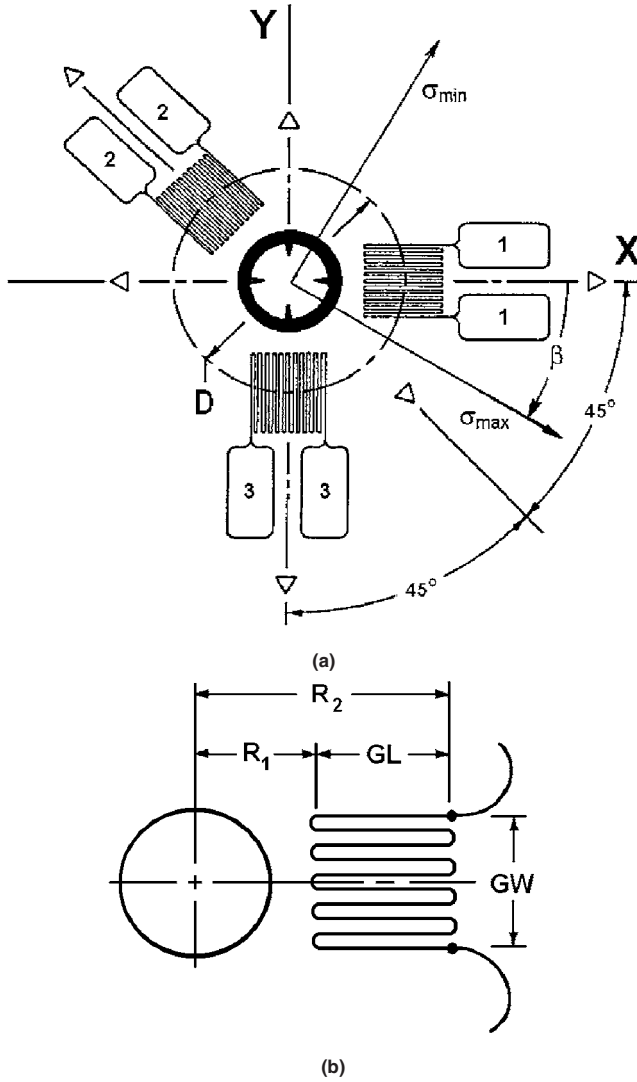


**FIG. 2 Schematic Geometry of a Typical Three-Element Clockwise (CW) Hole-Drilling Rosette, (a) Rosette Layout, (b) Detail of a Strain Gage**

(1-5)).<sup>3</sup> The relieved strains depend on the residual stresses that existed in the material originally within the hole.

4.4.2 For the uniform stress case shown in Fig. 1(a), the surface strain relief measured after hole-drilling is:

$$\begin{aligned} \epsilon = & \frac{1+\nu}{E} \bar{a} \frac{\sigma_x + \sigma_y}{2} \\ & + \frac{1}{E} \bar{b} \frac{\sigma_x - \sigma_y}{2} \cos 2\theta \\ & + \frac{1}{E} \bar{b} \tau_{xy} \sin 2\theta \end{aligned} \quad (1)$$

4.4.3 The calibration constants  $\bar{a}$  and  $\bar{b}$  indicate the relieved strains due to unit stresses within the hole depth. They are dimensionless, almost material-independent constants. Slightly different values of these constants apply for a through-

thickness hole made in a thin workpiece and for a blind hole made in a thick workpiece. Numerical values of these calibration constants have been determined from finite element calculations (4) for standard rosette patterns, and are tabulated in this test method.

4.4.4 For the non-uniform stress case shown in Fig. 1(b), the surface strain relief measured after completing hole depth step  $j$  depends on the residual stresses that existed in the material originally contained in all the hole depth steps  $1 \leq k \leq j$ :

$$\begin{aligned} \epsilon_j = & \frac{1+\nu}{E} \sum_{k=1}^j \bar{a}_{jk} ((\sigma_x + \sigma_y)/2)_k \\ & + \frac{1}{E} \sum_{k=1}^j \bar{b}_{jk} ((\sigma_x - \sigma_y)/2)_k \cos 2\theta \\ & + \frac{1}{E} \sum_{k=1}^j \bar{b}_{jk} (\tau_{xy})_k \sin 2\theta \end{aligned} \quad (2)$$

4.4.5 The calibration constants  $\bar{a}_{jk}$  and  $\bar{b}_{jk}$  indicate the relieved strains in a hole  $j$  steps deep, due to unit stresses within hole step  $k$ . Fig. 3 shows cross-sections of drilled holes for an example sequence where a hole is drilled in four depth steps. Within this sequence, calibration constant represents an intermediate stage where the hole has reached 3 steps deep, and has a unit stress acting within depth step 2. Numerical values of the calibration constants have been determined by finite element calculations (4) for standard rosette patterns, and are tabulated in this test method.

4.4.6 Measurement of the relieved strains after a series of hole depth steps provides sufficient information to calculate the stresses  $\sigma_x$ ,  $\sigma_y$  and  $\tau_{xy}$  within each step. From these stresses, the corresponding principal stresses  $\sigma_{\max}$  and  $\sigma_{\min}$  and their orientation  $\beta$  can be found.

4.4.7 The relieved strains are mostly influenced by the near-surface residual stresses. Interior stresses have influences that diminish with their depth from the surface. Thus, hole-drilling measurements can evaluate only near-surface stresses. Deep interior stresses cannot be identified reliably, see Note 7.

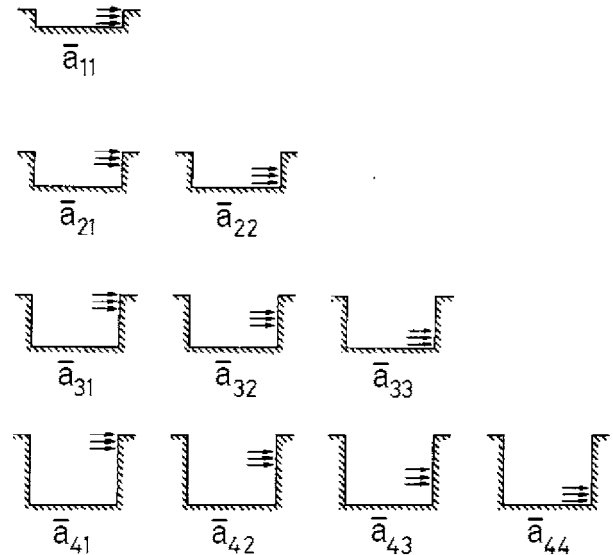


**FIG. 3 Physical Interpretation of Coefficients  $\bar{a}_{jk}$**

<sup>3</sup> The boldface numbers in parentheses refer to the list of references at the end of this standard.

4.4.8 In theory, it is possible for local yielding to occur due to the stress concentration around the drilled hole. Such yielding can occur with isotropic residual stresses exceeding 50 % of the yield stress, and for shear stresses exceeding 25 % of the yield stress. However, in practice it is found that satisfactory results can be achieved providing the residual stresses do not exceed about 60 % of the material yield stress (6).

## 5. Significance and Use

### 5.1 Summary:

5.1.1 Residual stresses are present in almost all materials. They may be created during the manufacture or during the life of the material. If not recognized and accounted for in the design process, residual stresses can be a major factor in the failure of a material, particularly one subjected to alternating service loads or corrosive environments. Residual stress may also be beneficial, for example, the compressive stresses produced by shot peening. The hole-drilling strain-gage technique is a practical method for determining residual stresses.

## 6. Workpiece Preparation

### 6.1 Requirements:

6.1.1 For a “thin” workpiece, where a through-hole is to be used, the workpiece thickness should not exceed 0.4D for a type A or B rosette, or 0.48D for a type C rosette (see Fig. 4).

6.1.2 For a “thick” workpiece, where a hole depth less than the workpiece thickness is to be used, the workpiece thickness should be at least 1.2D for a type A or B rosette, or 1.44D for a type C rosette (see Fig. 4).

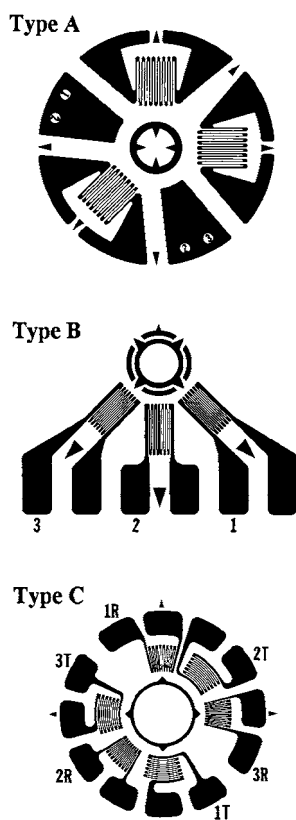


FIG. 4 Hole-Drilling Rosettes

6.1.3 A smooth surface is usually necessary for strain gage application. However, abrading or grinding that could appreciably alter the surface stresses must be avoided. Chemical etching could be used, thus avoiding the need for mechanical abrasion.

6.1.4 The surface preparation prior to bonding the strain gages shall conform to the recommendations of the manufacturer of the adhesive used to attach the strain gages. A thorough cleaning and degreasing is required. In general, surface preparation should be restricted to those methods that have been demonstrated to induce no significant residual surface stresses. This is particularly important for workpieces that contain sharp near-surface stress gradients.

## 7. Strain Gages and Instrumentation

### 7.1 Rosette Geometry:

7.1.1 A rosette comprising three single or pairs of strain gage grids shall be used. The numbering scheme for the strain gages follows a clockwise (CW) convention (7).

NOTE 2—The gage numbering scheme used for the rosette illustrated in Fig. 2 differs from the counter-clockwise (CCW) convention often used for general-purpose strain gage rosettes and for some other types of residual stress rosette. If a strain gage rosette with CCW gage numbering is used, the residual stress calculation procedure described in this test method still applies. The only changes are that the numbering of gages 1 and 3 are interchanged and that the angle  $\beta$  defining the direction of the most tensile principal stress  $\sigma_{\max}$  is reversed and is measured counter-clockwise from the new gage 1.

NOTE 3—It is recommended that the gages be calibrated in accordance with Test Methods E 251.

7.1.2 The gages shall be arranged in a circular pattern, equidistant from the center of the rosette.

7.1.3 The gage axes shall be oriented in each of three directions, (1) a reference direction, (2) 45° or 135° to the reference direction, and (3) perpendicular to the reference direction. Direction (2) bisects directions (1) and (3), as shown in Fig. 2.

7.1.4 The measurement direction of gage 1 in Fig. 1 is identified as the x-axis. The y-axis is 90° counterclockwise of the x-axis.

7.1.5 The center of the gage circle shall be clearly identifiable.

### 7.2 Standardized Rosettes:

7.2.1 Several different standardized rosettes are available to meet a wide range of residual stress measurement needs. The use of standardized rosette designs greatly simplifies the calculation of the residual stresses. Fig. 4 shows three different rosette types and Table 1 lists their dimensions.

7.2.2 The type A rosette shown in Fig. 4 was first introduced by Rendler and Vigness (5). This pattern is available in several different sizes, and is recommended for general-purpose use.

NOTE 4—Choice of rosette size is a primary decision. Larger rosettes tend to give more stable strain measurements because of their greater capacity to dissipate heat. They are also able to identify residual stresses to greater depths. Conversely, smaller rosettes can fit smaller workpieces, require smaller drilled holes, and give more localized measurements.

7.2.3 The type B rosette shown in Fig. 4 has all strain gage grids located on one side. It is useful where measurements need to be made near an obstacle.



**TABLE 1 Rosette Dimensions<sup>A</sup>**

Rosette Type	D	GL <sup>B</sup>	GW <sup>B</sup>	R <sub>1</sub> <sup>B</sup>	R <sub>2</sub> <sup>B</sup>
Type A					
Conceptual	D	0.309D	0.309D	0.3455D	0.6545D
1/32 in. nominal	0.101 (2.57)	0.031 (0.79)	0.031 (0.79)	0.035 (0.89)	0.066 (1.68)
1/16 in. nominal	0.202 (5.13)	0.062 (1.59)	0.062 (1.59)	0.070 (1.77)	0.132 (3.36)
1/8 in. nominal	0.404 (10.26)	0.125 (3.18)	0.125 (3.18)	0.140 (3.54)	0.264 (6.72)
Type B					
Conceptual	D	0.309D	0.223D	0.3455D	0.6545D
1/16 in. nominal	0.202 (5.13)	0.062 (1.59)	0.045 (1.14)	0.070 (1.77)	0.132 (3.36)
Type C					
Conceptual	D	0.176D	30° sector	0.412D	0.588D
1/16 in. nominal	0.170 (4.32)	0.030 (0.76)	30° (30°)	0.070 (1.78)	0.100 (2.54)

<sup>A</sup> Dimensions are in inches (mm).

<sup>B</sup> Rosette dimensions are defined in Fig. 2.

7.2.4 The type C rosette shown in Fig. 4 is a special-purpose pattern with three pairs of opposite strain gage grids that are to be connected as three half-bridges. It is useful where large strain sensitivity and high thermal stability are required (8).

#### 7.3 Installation and Use:

7.3.1 The strain gage rosette should be attached to the workpiece surface such that its center is at least 1.5D from the nearest edge, or the boundary of another material should the workpiece be comprised of more than one material.

7.3.2 When using a type B rosette adjacent to an obstacle, the center of the rosette should be at least 0.5D from the obstacle, with the set of strain gages diametrically opposite to the obstacle.

7.3.3 The application of the strain gage (bonding, wiring, protective coating) should closely follow the manufacturer's recommendations, and shall ensure the protection of the strain gage grid during the drilling operation.

7.3.4 The strain gages should remain permanently connected and the stability of the installation shall be verified. A resistance to ground of at least 20 000 MΩ is preferable.

7.3.5 Checks should be made to validate the integrity of the gage installation. If possible, a small mechanical load should be applied to the workpiece to induce some modest strains. The observed strains should return to zero when the load is removed. In addition, a visual inspection of the rosette installation should be made to check for possible areas that are not well bonded. If incomplete bonding is observed, the rosette must be removed and replaced.

#### 7.4 Instrumentation:

7.4.1 The instrumentation for recording of strains shall have a strain resolution of  $\pm 1 \times 10^{-6}$ , and stability and repeatability of the measurement shall be at least  $\pm 1 \times 10^{-6}$ . The lead wires from each gage should be as short as practicable and a three-wire temperature-compensating circuit (9) should be used with rosette types A and B. Half-bridge circuits should be

used with rosette type C, the resulting outputs of which are designated  $\epsilon_1$ ,  $\epsilon_2$ , and  $\epsilon_3$ .

## 8. Procedure

### 8.1 Suggested Preparatory Reading:

8.1.1 References (10) and (11) provide substantial practical guidance about how to make high-quality hole-drilling residual stress measurements. These publications are excellent preparatory reading, particularly for practitioners who infrequently make hole-drilling measurements.

### 8.2 Drilling Equipment and Use:

8.2.1 A device that is equipped to drill a hole in the test workpiece in a controlled manner is required. The device must be able to drill a hole aligned concentric with the strain gage circle to within either  $\pm 0.004D$ . It shall also be able to control the depth of the hole to within either  $\pm 0.004D$ . Fig. 5 illustrates a typical hole-drilling apparatus.

8.2.2 Several drilling techniques have been investigated and reported to be suitable for the hole drilling method. The most common drilling technique suitable for all but the hardest materials involves the use of carbide burs or endmills driven by a high-speed air turbine or electric motor rotating at 50 000 to 400 000 rpm (13). Low-speed drilling using a drill-press or power hand-drill is discouraged because the technique has the tendency to create machining-induced residual stresses at the hole boundary (14).

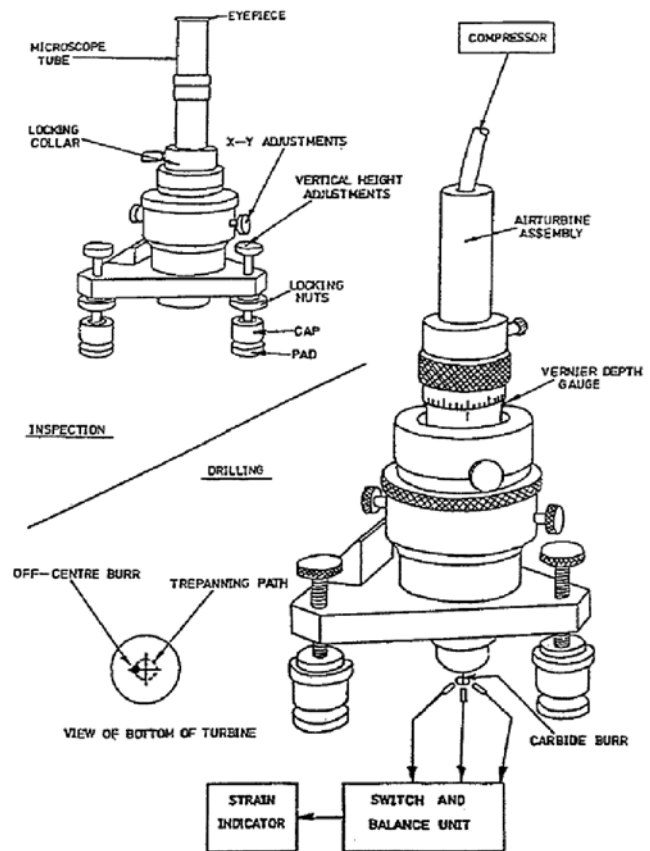


**FIG. 5 A Typical Hole-Drilling Apparatus, (a) Optical Device for Centering the Tool Holder, (b) Hole-Drilling Tool (from Owens (12))**

8.2.3 For very hard materials, abrasive jet machining can also be useful. This drilling method involves directing a high-velocity stream of air containing fine abrasive particles through a small-diameter nozzle against the workpiece (5, 14). Abrasive jet machining can be less suitable for softer materials (7). It should not be used for non-uniform stress measurements because the hole geometry and depth cannot be controlled sufficiently tightly.

8.2.4 When using burs or endmills, carbide “inverted cone” dental burs or small carbide endmills can be suitable as cutting tools. Commercially available cutters are designed for a wide range of applications, and not all types may be suited for hole drilling residual stress measurements. Thus, a verification of drilling technique and choice of cutter should be done when no prior experience is available. Verification could consist of applying a strain gage rosette to a stress-free workpiece of the same nominal test material produced by the annealing heat treatment method (1, 5, 14, 15), and then drilling a hole. If the drilling technique and cutter are satisfactory, the strains produced by the drilling will be small, typically within  $\pm 8 \mu\epsilon$ .

8.2.5 If the drilling technique verification shows significant strains induced by the drilling process, or if the test material is known to be difficult to machine, it may be helpful to lubricate the drilling cutter with a suitable lubricating fluid. The fluid used must be electrically non-conductive. Aqueous or other electrically conductive lubricants must not be used because they may penetrate the strain gage electrical connections and distort the strain readings.

8.2.6 The radial clearance angles of the cutting edges on the end face of the cutting tool should not exceed  $1^\circ$ . This requirement avoids ambiguities in hole depth identification by ensuring that the depth is uniform within 1 % of the tool diameter.

8.2.7 “Inverted cone” cutters have their maximum diameter at their end face, tapering slightly towards the shank. The tapered geometry provides clearance for the cylindrical cutting edges as the tool cuts the hole. This feature is desirable because it minimizes tool rubbing on the side surface of the hole and possible localized residual stress creation. To avoid ambiguities in hole diameter identification, the taper angle should not exceed  $5^\circ$  on each side.

8.2.8 Drilling may be done by plunging, where the cutter is advanced axially. Alternatively, an orbiting technique (16) may be used, where the rotation axis of the cutter is deliberately offset from the hole axis. The cutter is advanced axially, and is then orbited so that the offset traces a circular path and the cutter creates a hole larger than its diameter. The direct plunge method has the advantage of simplicity. The orbiting method has the advantages of hole diameter adjustment through choice of offset, use of the cylindrical cutting edges as well as those on the end surface, and clearer chip flow.

8.2.9 Table 2 indicates the target hole diameter ranges appropriate for the various rosette types. Different ranges apply to uniform and non-uniform stress measurements.

8.2.10 The size of the measured strains increases approximately proportionally with the square of the hole diameter. Thus, holes at the larger end of the range are preferred. If using the plunging method, the cutter diameter should equal the target diameter. If using the orbiting method, the cutter diameter should be 60 to 90 % of the target diameter, with an offset chosen to achieve a hole with the target diameter.

8.2.11 All drilling should be done under constant temperature conditions. After each drilling step, the cutter should be stopped to allow time for stabilization of any temperature fluctuations caused by the drilling process and air turbine

**TABLE 2 Recommended Workpiece Thicknesses, Hole Diameters and Depth Steps<sup>A</sup>**

Rosette Type	D	Max. thickness of a “Thin” workpiece	Min. thickness of a “Thick” workpiece	Uniform Stresses			Non-Uniform Stresses		
				Min. hole diameter	Max. hole diameter	Practical depth steps <sup>B</sup>	Min. hole diameter	Max. hole diameter	Practical depth steps <sup>B</sup>
Type A									
Conceptual	D	0.4 D	1.2 D	0.6 Max D <sub>0</sub>	Max D <sub>0</sub>	0.05 D	Min D <sub>0</sub>	Max D <sub>0</sub>	0.01 D
1/32 in. nominal	0.101 (2.57)	0.040 (1.03)	0.121 (3.08)	0.024 (0.61)	0.040 (1.01)	0.005 (0.25)	0.037 (0.93)	0.040 (1.00)	0.001 (0.025)
1/16 in. nominal	0.202 (5.13)	0.081 (2.06)	0.242 (6.17)	0.060 (1.52)	0.100 (2.54)	0.010 (0.25)	0.075 (1.88)	0.085 (2.12)	0.002 (0.05)
1/8 in. nominal	0.404 (10.26)	0.162 (4.11)	0.485 (12.34)	0.132 (3.35)	0.220 (5.59)	0.020 (0.50)	0.150 (3.75)	0.170 (4.25)	0.004 (0.10)
Type B									
Conceptual	D	0.4 D	1.2 D	0.6 Max D <sub>0</sub>	Max D <sub>0</sub>	0.05 D	Min D <sub>0</sub>	Max D <sub>0</sub>	0.01D
1/16 in. nominal	0.202 (5.13)	0.081 (2.06)	0.242 (6.17)	0.060 (1.52)	0.100 (2.54)	0.010 (0.25)	0.075 (1.88)	0.085 (2.12)	0.002 (0.05)
Type C									
Conceptual	D	0.48 D	1.44 D	0.6 Max D <sub>0</sub>	Max D <sub>0</sub>	0.0575 D	Min D <sub>0</sub>	Max D <sub>0</sub>	0.0115 D
1/16 in. nominal	0.170 (4.32)	0.082 (2.07)	0.245 (6.22)	0.060 (1.52)	0.100 (2.54)	0.010 (0.25)	0.075 (1.88)	0.085 (2.12)	0.002 (0.05)

<sup>A</sup> Dimensions are in inches (mm).

<sup>B</sup> See Note 6.



exhaust. It is not essential to retract the cutter. Strain readings should attain their final values for at least five seconds before being accepted.

8.2.12 Use the drilling procedure described in 8.3 when evaluating uniform stresses in a “thin” workpiece, in 8.4 for uniform stresses in a “thick” workpiece, and in 8.5 for non-uniform stresses in a “thick” workpiece.

8.3 *Drilling Procedure for a “Thin” Workpiece with Uniform Stresses:*

8.3.1 For a “thin” workpiece, as defined in 6.1.1, obtain an initial reading from each gage before starting the drilling operation.

8.3.2 Start the cutter and slowly advance it until it cuts through the entire thickness of the workpiece. If using the orbiting technique, also orbit the cutter. Stop and retract the cutter. Then measure one set of strain readings  $\epsilon_1$ ,  $\epsilon_2$  and  $\epsilon_3$ .

8.3.3 Measure the hole diameter and confirm that it lies within the target range specified in Table 2.

8.3.4 Check the hole concentricity and confirm that it lies within the tolerance specified in 8.2.1.

8.3.5 Compute uniform residual stresses as described in 9.1.

8.4 *Drilling Procedure for a “Thick” Workpiece with Uniform Stresses:*

8.4.1 For a “thick” workpiece, as defined in 6.1.2, obtain an initial reading from each gage before starting the drilling operation. Start the cutter and slowly advance it until it cuts through the rosette backing material and lightly scratches the workpiece surface. This point corresponds to “zero” cutter depth.

NOTE 5—Some practitioners use a technique that identifies the “zero” point by the completion of an electrical connection between the cutter and the workpiece.

8.4.2 Stop the cutter after reaching the “zero” point and confirm that all strain gage readings have not significantly changed. Use the new readings as the zero points for the subsequent strain measurements.

8.4.3 Start the cutter and advance it by 0.05 D for a type A or B rosette, or 0.06D for a type C rosette. If using the orbiting technique, also orbit the cutter. Stop the cutter and record the readings from each strain gage,  $\epsilon_1$ ,  $\epsilon_2$  and  $\epsilon_3$ . Other similar depth increments are acceptable; however, they are less convenient for calculations because they will require additional interpolations of the calibration constants listed in Table 3.

NOTE 6—For practical measurements, the required cutter advance can be approximated as 0.005 in. (0.125 mm) for a  $1/32$  in. Type A rosette, 0.010 in. (0.25 mm) for a  $1/16$  in. Type A, B or C rosette, or 0.020 in. (0.5 mm) for a  $1/8$  in. Type A rosette (see Table 2). The associated small deviations from the specified 0.05D or 0.06D values do not significantly affect the calculated residual stress results.

8.4.4 Repeat the stepwise advance in hole depth followed by strain measurements to a total of 8 equal hole depth steps, reaching a final hole depth approximately equal to 0.4D for a type A or B rosette, or 0.48D for a type C rosette.

NOTE 7—A final depth of 0.4D or 0.48D is used because the measured strains continue to increase until this depth is reached. However, the measured strains mostly depend on the near-surface stresses, with sensitivity diminishing to near zero for stresses beyond 0.2D depth with Type A and B rosettes, or 0.3D depth with a Type C rosette. Thus, hole-drilling

measurements indicate a weighted average of the residual stresses within the near-surface layer, 0.2D or 0.3D deep from the measured surface.

8.4.5 Measure the hole diameter and confirm that it lies within the target range specified in Table 2.

8.4.6 Check the hole concentricity and confirm that it lies within the tolerance specified in 8.2.1.

8.4.7 Compute uniform residual stresses as described in 9.2.

8.5 *Drilling Procedure for a “Thick” Workpiece with Non-Uniform Stresses:*

8.5.1 Obtain zero readings from each gage before starting the drilling operation. Start the cutter and carefully advance it until it cuts through the rosette backing material and lightly scratches the workpiece surface. This point corresponds to “zero” cutter depth (see Note 5).

8.5.2 Stop the cutter after reaching the “zero” point and confirm that all strain gage readings have not significantly changed. Use the new readings as the zero points for the subsequent strain measurements.

8.5.3 Start the cutter and advance it by 0.001 in. (0.025 mm) for a  $1/32$  in. Type A Rosette, 0.002 in. (0.05 mm) for a  $1/16$  in. Type A, B or C Rosette, or 0.004 in. (0.10 mm) for a  $1/8$  in. Type A Rosette. Stop the cutter and record the readings from each strain gage.

8.5.4 When working with a Type A or B Rosette, repeat the stepwise advance in hole depth followed by strain measurements to a total of 20 equal hole depth steps.

8.5.5 When working with a Type C Rosette, repeat the stepwise advance in hole depth followed by strain measurements to a total of 25 equal hole depth steps.

8.5.6 Measure the hole diameter and confirm that it lies within the target range specified in Table 2.

8.5.7 Check the hole concentricity and confirm that it lies within the tolerance specified in 8.2.1.

8.5.8 Compute non-uniform residual stresses as described in Section 10.

## 9. Computation of Uniform Stresses

9.1 *“Thin” Workpiece:*

9.1.1 Compute the following combination strains for the measured strains  $\epsilon_1$ ,  $\epsilon_2$ ,  $\epsilon_3$ :

$$p = (\epsilon_3 + \epsilon_1) / 2 \quad (3)$$

$$q = (\epsilon_3 - \epsilon_1) / 2 \quad (4)$$

$$t = (\epsilon_3 + \epsilon_1 - 2\epsilon_2) / 2 \quad (5)$$

9.1.2 Use Table 3 to determine the numerical values of the calibration constants  $\bar{a}$  and  $\bar{b}$  corresponding to the hole diameter and type of rosette used.

9.1.3 Compute the three combination stresses  $P$ ,  $Q$  and  $T$  corresponding to the three combination strains  $p$ ,  $q$  and  $t$  using (4):

$$P = \frac{\sigma_y + \sigma_x}{2} = -\frac{E p}{\bar{a}(1 + \nu)} \quad (6)$$

$$Q = \frac{\sigma_y - \sigma_x}{2} = -\frac{E q}{\bar{b}} \quad (7)$$

$$T = \tau_{xy} = -\frac{E t}{\bar{b}} \quad (8)$$

**TABLE 3 Numerical Values of Coefficients  $\bar{a}$  and  $\bar{b}$  for Uniform Stress Evaluations**

Rosette A	$\bar{a}$					$\bar{b}$				
Blind hole	Hole Diameter, $D_o/D$					Hole Diameter, $D_o/D$				
Depth/D	0.30	0.35	0.40	0.45	0.50	0.30	0.35	0.40	0.45	0.50
0.00	.000	.000	.000	.000	.000	.000	.000	.000	.000	.000
0.05	.027	.037	.049	.063	.080	.051	.069	.090	.113	.140
0.10	.059	.081	.108	.138	.176	.118	.159	.206	.255	.317
0.15	.085	.115	.151	.192	.238	.180	.239	.305	.375	.453
0.20	.101	.137	.177	.223	.273	.227	.299	.377	.459	.545
0.25	.110	.147	.190	.238	.288	.259	.339	.425	.513	.603
0.30	.113	.151	.195	.243	.293	.279	.364	.454	.546	.638
0.35	.113	.151	.195	.242	.292	.292	.379	.472	.566	.657
0.40	.111	.149	.192	.239	.289	.297	.387	.482	.576	.668
Through Hole	.090	.122	.160	.203	.249	.288	.377	.470	.562	.651
Rosette B	$\bar{a}$					$\bar{b}$				
Blind Hole	Hole Diameter, $D_o/D$					Hole Diameter, $D_o/D$				
Depth/D	0.30	0.35	0.40	0.45	0.50	0.30	0.35	0.40	0.45	0.50
0.00	.000	.000	.000	.000	.000	.000	.000	.000	.000	.000
0.05	.029	.039	.053	.068	.086	.058	.078	.102	.127	.157
0.10	.063	.087	.116	.148	.189	.134	.179	.231	.286	.355
0.15	.090	.123	.162	.205	.254	.203	.269	.343	.419	.504
0.20	.107	.145	.189	.236	.289	.256	.336	.423	.511	.605
0.25	.116	.156	.202	.251	.305	.292	.381	.476	.571	.668
0.30	.120	.160	.206	.256	.309	.315	.410	.509	.609	.707
0.35	.120	.160	.206	.256	.308	.330	.427	.529	.631	.730
0.40	.118	.158	.203	.253	.305	.337	.437	.541	.644	.743
Through Hole	.096	.131	.171	.216	.265	.329	.428	.531	.630	.725
Rosette C	$\bar{a}$					$\bar{b}$				
Blind Hole	Hole Diameter, $D_o/D$					Hole Diameter, $D_o/D$				
Depth/D	0.40	0.45	0.50	0.55	0.60	0.40	0.45	0.50	0.55	0.60
0.00	.000	.000	.000	.000	.000	.000	.000	.000	.000	.000
0.06	.081	.106	.132	.163	.200	.132	.167	.199	.235	.279
0.12	.178	.230	.286	.349	.427	.309	.386	.451	.533	.624
0.18	.252	.321	.395	.475	.565	.464	.569	.666	.760	.857
0.24	.297	.375	.458	.546	.640	.576	.696	.805	.905	.997
0.30	.321	.404	.491	.583	.679	.650	.778	.893	.994	1.081
0.36	.333	.417	.507	.601	.701	.697	.829	.946	1.048	1.131
0.42	.337	.422	.514	.610	.712	.727	.860	.980	1.082	1.162
0.48	.338	.423	.516	.614	.717	.746	.881	1.001	1.103	1.182
Through Hole	.316	.399	.494	.597	.707	.623	.723	.799	.847	.859

where:

$P$  = isotropic (equi-biaxial) stress,

$Q$  = 45° shear stress, and

$T$  = xy shear stress.

9.1.4 Compute the in-plane Cartesian stresses  $\sigma_x$ ,  $\sigma_y$  and  $\tau_{xy}$  using:

$$\sigma_x = P - Q \quad (9)$$

$$\sigma_y = P + Q \quad (10)$$

$$\tau_{xy} = T \quad (11)$$

9.1.5 Compute the principal stresses  $\sigma_{\max}$  and  $\sigma_{\min}$  using:

$$\sigma_{\max}, \sigma_{\min} = P \pm \sqrt{Q^2 + T^2} \quad (12)$$

9.1.6 The more tensile (or less compressive) principal stress  $\sigma_{\max}$  is located at an angle  $\beta$  measured clockwise from the direction of gage 1 in Fig. 2. Similarly, the less tensile (or more compressive) principal stress  $\sigma_{\min}$  is located at an angle  $\beta$  measured clockwise from the direction of gage 3.

9.1.7 Compute the angle  $\beta$  using:

$$\beta = \frac{1}{2} \arctan\left(\frac{-T}{-Q}\right) \quad (13)$$

9.1.8 Calculation of the angle  $\beta$  using the common one-argument arctan function, such as is found on an ordinary calculator, can give an ambiguity of  $\pm 90^\circ$ . The correct angle can be found by using the two-argument arctan function (function atan2 in some computer languages), where the signs of the numerator and denominator are each taken into account. Alternatively, the result from the one-argument calculation can be adjusted by adding or subtracting  $90^\circ$  as necessary to place  $\beta$  within the appropriate range defined in Table 4.

9.1.9 A positive value of  $\beta$ , say  $\beta = 30^\circ$ , indicates that  $\sigma_{\max}$  lies  $30^\circ$  clockwise of the direction of gage 1. A negative value of  $\beta$ , say  $\beta = -30^\circ$ , indicates that  $\sigma_{\max}$  lies  $30^\circ$  counter-clockwise of the direction of gage 1. In general, the direction

**TABLE 4 Placement of the Principal Angle  $\beta$** 

	$Q > 0$	$Q = 0$	$Q < 0$
$T < 0$	$45^\circ < \beta < 90^\circ$	$45^\circ$	$0^\circ < \beta < 45^\circ$
$T = 0$	$90^\circ$	undefined	$0^\circ$
$T > 0$	$-90^\circ < \beta < -45^\circ$	$-45^\circ$	$-45^\circ < \beta < 0^\circ$



of  $\sigma_{\max}$  will closely correspond to the direction of the numerically most negative (compressive) relieved strain.

NOTE 8—The clockwise (CW) measurement direction for angle  $\beta$  defined in 9.1.10 applies only to a strain gage rosette with CW gage numbering, such as that illustrated in Fig. 2. The opposite measurement direction for  $\beta$  applies to a counter-clockwise (CCW) strain gage rosette. In such a rosette, the geometrical locations of gages 1 and 3 are interchanged relative to the CW case. The new gage 1 becomes the reference gage. For a CCW rosette, a positive value of  $\beta$ , say  $\beta = 30^\circ$ , indicates that  $\sigma_{\max}$  lies  $30^\circ$  counter-clockwise of the direction of gage 1. All other aspects of the residual stress calculation are identical for both CW and CCW rosettes.

9.1.10 If either of the computed principal stresses exceeds 60 % of the material yield stress, then some localized yielding has occurred in the material around the hole. In this case, the results are not quantitative, and must be reported as “indicative” only. In general, the computed stresses whose values exceed 60 % of the material yield stress tend to be overestimated. Their actual values are usually smaller than indicated.

## 9.2 “Thick” Workpiece:

9.2.1 Plot graphs of strains  $\epsilon_1$ ,  $\epsilon_2$ ,  $\epsilon_3$  versus hole depth and confirm that the data follow generally smooth trends. Investigate substantial irregularities and obvious outliers. If necessary, repeat the hole-drilling test.

9.2.2 For each set of  $\epsilon_1$ ,  $\epsilon_2$ ,  $\epsilon_3$  measurements, calculate the corresponding combination strains  $p$ ,  $q$  and  $t$  using Eq 3-5.

9.2.3 Verify that the residual stresses are uniform within the hole depth. Identify the set of combination strains  $q$  or  $t$  that contains larger absolute values. Express each set of combination strains  $p$  and the larger of  $q$  and  $t$  as a percentage of their values at the maximum specified hole depth. Plot these percent strains versus hole depth. These graphs should yield data points very close to the curves shown in Fig. 6 (17). Data points that are significantly separated from the curves in Fig. 6, say by more than  $\pm 3\%$ , indicate either substantial stress non-uniformity through the material thickness, or strain measurement errors. In either case, the measured data are not acceptable for uniform residual stress calculations. Further measurements for non-uniform residual stresses may be appropriate, see 8.5.

NOTE 9—This graphical test is not a sensitive indicator of stress field uniformity. Workpieces with significantly non-uniform stress fields can yield percentage relieved strain curves substantially similar to those shown in Fig. 6. The main purpose of the test is to identify grossly non-uniform stress fields and strain measurement errors. This stress uniformity test is available only when working with “thick” workpieces.

9.2.4 For each of the hole depths corresponding to the eight sets of  $\epsilon_1$ ,  $\epsilon_2$ ,  $\epsilon_3$  measurements, use Table 3 to determine the numerical values of the calibration constants  $\bar{a}$  and  $\bar{b}$  corresponding to the hole depth and diameter, and the type of rosette used. The numerical values in this table derive from finite element analyses (4).

9.2.5 Compute the three combination stresses  $P$ ,  $Q$  and  $T$  corresponding to the three sets of combination strains  $p$ ,  $q$ , and  $t$  using the following formulas (18):

$$P = -\frac{E}{1+\nu} \frac{\sum (\bar{a} \cdot p)}{\sum (\bar{a}^2)} \quad (14)$$

## Rosette Types A & B

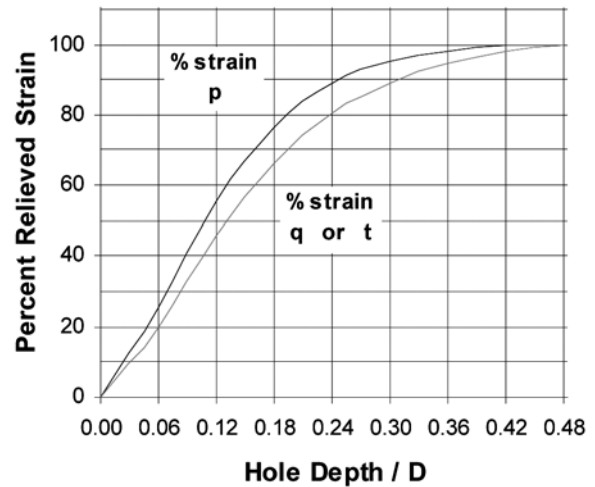
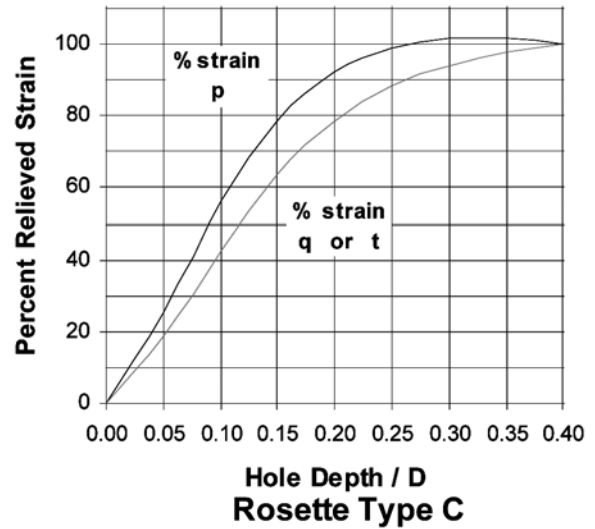


FIG. 6 Typical Plots of Percent of Strain versus Depth for Uniform Through-Thickness Stress, (a) Rosette Types A & B, (b) Rosette Type C

$$Q = -E \frac{\sum (\bar{b} \cdot q)}{\sum (\bar{b}^2)} \quad (15)$$

$$T = -E \frac{\sum (\bar{b} \cdot t)}{\sum (\bar{b}^2)} \quad (16)$$

where  $\Sigma$  indicates a summation of the indicated quantities for the eight hole depths.

NOTE 10—It is possible to evaluate the combination stresses  $P$ ,  $Q$  and  $T$  using Eq 3-8 with only one set of the  $\epsilon_1$ ,  $\epsilon_2$ ,  $\epsilon_3$  measurements, for example, the values at the maximum hole depth. Such a calculation could be useful to give a quick residual stress estimate. However, the averaging method used in 9.2.5 is preferred because it uses all the measured strain data, and it significantly reduces the effects of random strain measurement errors (19).

9.2.6 Compute the Cartesian stresses  $\sigma_x$ ,  $\sigma_y$  and  $\tau_{xy}$ , the principal stresses  $\sigma_{\max}$  and  $\sigma_{\min}$ , and the principal angle  $\beta$  as described in 9.1.5 to 9.1.10.

## 9.3 Intermediate Thickness Workpieces:

9.3.1 The intermediate case of a workpiece whose thickness lies between the specifications for “thin” and “thick” workpieces is outside the scope of this test method. For workpieces with uniform stress, an approximate result can be obtained for such workpieces by using a through hole and interpolating the “Blind Hole” and “Through-the-thickness Hole” calibration data given in Table 3. Residual stress results obtained in this way should be reported as “nonstandard” and “approximate.”

## 10. Computation of Non-Uniform Stresses

### 10.1 Strain Data:

10.1.1 Plot graphs of strains  $\epsilon_1$ ,  $\epsilon_2$ ,  $\epsilon_3$  versus hole depth and confirm that the data follow generally smooth trends. Investigate substantial irregularities and obvious outliers. If necessary, repeat the hole-drilling test.

10.1.2 Compute the following combination strain vectors for each set of measured strains,  $\epsilon_1$ ,  $\epsilon_2$ ,  $\epsilon_3$ :

$$p_j = (\epsilon_3 + \epsilon_1)_j / 2 \quad (17)$$

$$q_j = (\epsilon_3 - \epsilon_1)_j / 2 \quad (18)$$

$$t_j = (\epsilon_3 + \epsilon_1 - 2\epsilon_2)_j / 2 \quad (19)$$

where the subscript  $j$  refers to the serial numbers of the hole depth steps corresponding to the successive sets of measured strains  $\epsilon_1$ ,  $\epsilon_2$ ,  $\epsilon_3$ .

10.1.3 Estimate the standard errors in the combination strains (20):

$$p_{std}^2 = \sum_{j=1}^{n-3} \frac{(p_j - 3p_{j+1} + 3p_{j+2} - p_{j+3})^2}{20(n-3)} \quad (20)$$

$$q_{std}^2 = \sum_{j=1}^{n-3} \frac{(q_j - 3q_{j+1} + 3q_{j+2} - p_{j+3})^2}{20(n-3)} \quad (21)$$

$$t_{std}^2 = \sum_{j=1}^{n-3} \frac{(t_j - 3t_{j+1} + 3t_{j+2} - t_{j+3})^2}{20(n-3)} \quad (22)$$

where  $n$  = the number of sets of strain data at the various hole depth steps. The summation is carried out over the range  $1 \leq j \leq n - 3$ .

### 10.2 Calibration Matrices:

10.2.1 If using a type A rosette, use the calibration data given in Table 5 to form the matrices  $\bar{a}_{jk}$  and  $\bar{b}_{jk}$ . The tabulated numbers refer to a  $1/16$  in. nominal size rosette, which is the most commonly used size. If using a  $1/32$  in. rosette, multiply all hole and stress depths in the table by 0.5. If using a  $1/8$  in. rosette, multiply all hole and stress depths by 2.

10.2.2 If using a type B rosette, use the calibration data given in Table 6 to form the matrices  $\bar{a}_{jk}$  and  $\bar{b}_{jk}$ . If using a type C rosette, use Table 7 instead. Types B and C rosettes are generally available only in  $1/16$  in. nominal size.

10.2.3 The tabulated numbers in Tables 5-7 correspond to a hole diameter of 0.080 in. (2 mm). Adjust the numbers to conform to the measured hole diameter by multiplying them by (measured hole diameter/0.080 in.)<sup>2</sup> or (measured hole diameter/2 mm)<sup>2</sup> as appropriate.

NOTE 11—The small discrepancies between the quoted inch and millimeter dimensions are not significant, and may be ignored.

NOTE 12—The numbers in Tables 5-7 are listed with five decimal places to reduce round-off errors when doing calculations using an entire matrix of numbers. This format exceeds the expected precision of any individual number.

### 10.3 Stress Calculation Method:

10.3.1 Using the Integral Method (4), the residual stresses within each hole depth step can be computed from the corresponding measured strains by solving the matrix equations:<sup>4</sup>

$$\bar{\mathbf{a}} \mathbf{P} = \frac{E}{1 + \nu} \mathbf{p} \quad (23)$$

$$\bar{\mathbf{b}} \mathbf{Q} = E \mathbf{q} \quad (24)$$

$$\bar{\mathbf{b}} \mathbf{T} = E \mathbf{t} \quad (25)$$

in which:

$$P_k = ((\sigma_y)_k + (\sigma_x)_k) / 2 \quad (26)$$

$$Q_k = ((\sigma_y)_k + (\sigma_x)_k) / 2 \quad (27)$$

$$T_k = (\tau_{xy})_k \quad (28)$$

and where the combination strains  $\mathbf{p}$ ,  $\mathbf{q}$  and  $\mathbf{t}$  are as defined in Eq 17-19. Stress calculations using Eq 23-25 are effective when few hole depth steps are used (4). However, for the large number of hole depth depths used here, the matrices  $\mathbf{a}$  and  $\mathbf{b}$  become numerically ill-conditioned. Under these conditions, small errors in the measured strains cause proportionally larger errors in the calculated stresses. To reduce this effect, use Tikhonov regularization (20-22) as described in the following paragraphs.

10.3.2 Form the tri-diagonal “second derivative” matrix  $\mathbf{c}$ :

$$\mathbf{c} = \begin{bmatrix} 0 & 0 & & & \\ -1 & 2 & -1 & & \\ & -1 & 2 & -1 & \\ & & -1 & 2 & -1 \\ & & & 0 & 0 \end{bmatrix} \quad (29)$$

where the number of rows equals the number of hole depth steps used. The first and last rows contain zeros; all other rows have  $[-1 \ 2 \ -1]$  centered along the diagonal.

10.3.3 Augment Eq 23-25 using matrix  $\mathbf{c}$  to implement Tikhonov second-derivative (smooth model) regularization:

$$(\bar{\mathbf{a}}^T \bar{\mathbf{a}} + \alpha_P \mathbf{c}^T \mathbf{c}) \mathbf{P} = \frac{E}{1 + \nu} \bar{\mathbf{a}}^T \mathbf{p} \quad (30)$$

$$(\bar{\mathbf{b}}^T \bar{\mathbf{b}} + \alpha_Q \mathbf{c}^T \mathbf{c}) \mathbf{Q} = E \bar{\mathbf{b}}^T \mathbf{q} \quad (31)$$

$$(\bar{\mathbf{b}}^T \bar{\mathbf{b}} + \alpha_T \mathbf{c}^T \mathbf{c}) \mathbf{T} = E \bar{\mathbf{b}}^T \mathbf{t} \quad (32)$$

10.3.4 The factors  $\alpha_P$ ,  $\alpha_Q$  and  $\alpha_T$  control the amount of regularization that is used. Regularization has the effect of smoothing the stress results. Zero values for the factors make Eq 30-32 equivalent to the unregularized Eq 23-25. Positive values of the factors give regularization (smoothing) amounts that increase as larger factors are chosen. Insufficient regularization leaves excessive noise in the calculated stress results, while excessive regularization distorts the stress results. Optimal regularization balances these two tendencies.

10.3.5 Make initial guesses for the required values  $\alpha_P$ ,  $\alpha_Q$  and  $\alpha_T$ . Small numbers in the range  $10^{-4}$  to  $10^{-6}$  are suitable. Solve Eq 30-32 to determine the stresses  $\mathbf{P}$ ,  $\mathbf{Q}$  and  $\mathbf{T}$ .

<sup>4</sup> Boldface type in equations indicates matrix and vector quantities. Thus  $\bar{\mathbf{a}}$  represents the set of quantities  $\bar{a}_{jk}$ , etc.



TABLE 5

Table 5(a) Hole-Drilling Calibration Matrix  $\bar{a}$  for a  $\frac{1}{16}$  in. Type A Rosette with a 0.080 in. (2 mm) Hole<sup>a</sup>

		Stress Depth									
Hole Depth in.	mm	0.002 0.05	0.004 0.10	0.006 0.15	0.008 0.20	0.010 0.25	0.012 0.30	0.014 0.35	0.016 0.40	0.018 0.45	0.020 in. 0.50 mm
0.002	0.05	-0.00679									
0.004	0.10	-0.00815	-0.00714								
0.006	0.15	-0.00937	-0.00844	-0.00734							
0.008	0.20	-0.01046	-0.00960	-0.00858	-0.00739						
0.010	0.25	-0.01141	-0.01063	-0.00968	-0.00856	-0.00728					
0.012	0.30	-0.01223	-0.01152	-0.01064	-0.00960	-0.00839	-0.00701				
0.014	0.35	-0.01291	-0.01227	-0.01147	-0.01050	-0.00936	-0.00806	-0.00659			
0.016	0.40	-0.01360	-0.01287	-0.01207	-0.01132	-0.01015	-0.00893	-0.00759	-0.00615		
0.018	0.45	-0.01416	-0.01344	-0.01264	-0.01184	-0.01082	-0.00970	-0.00846	-0.00712	-0.00567	
0.020	0.50	-0.01463	-0.01392	-0.01312	-0.01223	-0.01134	-0.01031	-0.00917	-0.00793	-0.00657	-0.00511
0.022	0.55	-0.01508	-0.01434	-0.01354	-0.01270	-0.01173	-0.01072	-0.00977	-0.00854	-0.00730	-0.00600
0.024	0.60	-0.01545	-0.01471	-0.01391	-0.01306	-0.01211	-0.01113	-0.01013	-0.00906	-0.00791	-0.00670
0.026	0.65	-0.01578	-0.01503	-0.01422	-0.01340	-0.01243	-0.01146	-0.01049	-0.00938	-0.00842	-0.00722
0.028	0.70	-0.01606	-0.01531	-0.01450	-0.01366	-0.01271	-0.01175	-0.01078	-0.00970	-0.00869	-0.00765
0.030	0.75	-0.01629	-0.01554	-0.01473	-0.01390	-0.01294	-0.01199	-0.01102	-0.00996	-0.00892	-0.00795
0.032	0.80	-0.01649	-0.01574	-0.01493	-0.01410	-0.01313	-0.01217	-0.01123	-0.01018	-0.00919	-0.00815
0.034	0.85	-0.01665	-0.01590	-0.01510	-0.01426	-0.01330	-0.01234	-0.01138	-0.01036	-0.00938	-0.00836
0.036	0.90	-0.01679	-0.01604	-0.01523	-0.01441	-0.01344	-0.01248	-0.01151	-0.01049	-0.00955	-0.00852
0.038	0.95	-0.01692	-0.01617	-0.01536	-0.01452	-0.01357	-0.01261	-0.01164	-0.01063	-0.00967	-0.00866
0.040	1.00	-0.01704	-0.01628	-0.01548	-0.01465	-0.01368	-0.01272	-0.01176	-0.01074	-0.00978	-0.00877

		Stress Depth									
Hole Depth in.	mm	0.022 0.55	0.024 0.60	0.026 0.65	0.028 0.70	0.030 0.75	0.032 0.80	0.034 0.85	0.036 0.90	0.038 0.95	0.040 in. 1.00 mm
0.022	0.55	-0.00464									
0.024	0.60	-0.00543	-0.00411								
0.026	0.65	-0.00604	-0.00485	-0.00364							
0.028	0.70	-0.00655	-0.00544	-0.00431	-0.00316						
0.030	0.75	-0.00693	-0.00589	-0.00484	-0.00378	-0.00270					
0.032	0.80	-0.00716	-0.00624	-0.00524	-0.00425	-0.00328	-0.00231				
0.034	0.85	-0.00738	-0.00644	-0.00555	-0.00464	-0.00373	-0.00283	-0.00195			
0.036	0.90	-0.00755	-0.00665	-0.00574	-0.00492	-0.00406	-0.00323	-0.00241	-0.00162		
0.038	0.95	-0.00770	-0.00679	-0.00592	-0.00508	-0.00432	-0.00353	-0.00277	-0.00203	-0.00131	
0.040	1.00	-0.00781	-0.00690	-0.00605	-0.00521	-0.00448	-0.00374	-0.00303	-0.00234	-0.00167	-0.00103

Table 5(b) Hole-Drilling Calibration Matrix  $\bar{b}$  for a  $\frac{1}{16}$  in. Type A Rosette with a 0.080 in. (2 mm) Hole<sup>a</sup>

		Stress Depth									
Hole Depth in.	mm	0.002 0.05	0.004 0.10	0.006 0.15	0.008 0.20	0.010 0.25	0.012 0.30	0.014 0.35	0.016 0.40	0.018 0.45	0.020 in. 0.50 mm
0.002	0.05	-0.01264									
0.004	0.10	-0.01470	-0.01352								
0.006	0.15	-0.01656	-0.01554	-0.01414							
0.008	0.20	-0.01821	-0.01735	-0.01611	-0.01449						
0.010	0.25	-0.01967	-0.01897	-0.01789	-0.01642	-0.01458					
0.012	0.30	-0.02092	-0.02038	-0.01946	-0.01815	-0.01647	-0.01439				
0.014	0.35	-0.02197	-0.02159	-0.02083	-0.01968	-0.01815	-0.01624	-0.01395			
0.016	0.40	-0.02308	-0.02256	-0.02182	-0.02112	-0.01952	-0.01778	-0.01576	-0.01348		
0.018	0.45	-0.02400	-0.02351	-0.02280	-0.02202	-0.02072	-0.01917	-0.01735	-0.01525	-0.01289	
0.020	0.50	-0.02481	-0.02434	-0.02366	-0.02273	-0.02167	-0.02031	-0.01868	-0.01678	-0.01460	-0.01216
0.022	0.55	-0.02554	-0.02507	-0.02440	-0.02362	-0.02235	-0.02103	-0.01981	-0.01793	-0.01599	-0.01386
0.024	0.60	-0.02616	-0.02571	-0.02505	-0.02428	-0.02305	-0.02177	-0.02045	-0.01890	-0.01715	-0.01522
0.026	0.65	-0.02668	-0.02625	-0.02561	-0.02487	-0.02364	-0.02239	-0.02109	-0.01949	-0.01813	-0.01623
0.028	0.70	-0.02715	-0.02673	-0.02611	-0.02536	-0.02417	-0.02294	-0.02164	-0.02012	-0.01866	-0.01708
0.030	0.75	-0.02753	-0.02713	-0.02653	-0.02582	-0.02463	-0.02341	-0.02213	-0.02064	-0.01911	-0.01767
0.032	0.80	-0.02789	-0.02749	-0.02690	-0.02620	-0.02502	-0.02382	-0.02256	-0.02108	-0.01968	-0.01807
0.034	0.85	-0.02821	-0.02781	-0.02722	-0.02652	-0.02536	-0.02417	-0.02292	-0.02146	-0.02007	-0.01850
0.036	0.90	-0.02848	-0.02809	-0.02750	-0.02682	-0.02565	-0.02447	-0.02324	-0.02176	-0.02041	-0.01885
0.038	0.95	-0.02871	-0.02832	-0.02774	-0.02706	-0.02591	-0.02473	-0.02350	-0.02204	-0.02067	-0.01916
0.040	1.00	-0.02889	-0.02851	-0.02794	-0.02727	-0.02612	-0.02495	-0.02373	-0.02227	-0.02089	-0.01940

		Stress Depth									
Hole Depth in.	mm	0.022 0.55	0.024 0.60	0.026 0.65	0.028 0.70	0.030 0.75	0.032 0.80	0.034 0.85	0.036 0.90	0.038 0.95	0.040 in. 1.00 mm
0.022	0.55	-0.01156									
0.024	0.60	-0.01310	-0.01081								
0.026	0.65	-0.01430	-0.01226	-0.01013							
0.028	0.70	-0.01531	-0.01345	-0.01149	-0.00944						
0.030	0.75	-0.01608	-0.01439	-0.01260	-0.01073	-0.00875					

TABLE 5 Continued

0.032	0.80	-0.01652	-0.01511	-0.01344	-0.01172	-0.00995	-0.00812				
0.034	0.85	-0.01698	-0.01549	-0.01408	-0.01251	-0.01089	-0.00921	-0.00747			
0.036	0.90	-0.01736	-0.01590	-0.01441	-0.01312	-0.011591	-0.01004	-0.00847	-0.00688		
0.038	0.95	-0.01769	-0.01624	-0.01480	-0.01340	-0.01213	-0.01072	-0.00928	-0.00781	-0.00632	
0.040	1.00	-0.01796	-0.01655	-0.01511	-0.01367	-0.01249	-0.01121	-0.00989	-0.00856	-0.00719	-0.00581

<sup>A</sup> Data are for a 1/16 in. rosette. Multiply hole and stress depths by 0.5 for a 1/32 in. rosette, and by 2 for a 1/8 in. rosette.

10.3.6 Because of the regularization used, the unregularized strains that correspond to the calculated stresses **P**, **Q** and **T** through Eq 23-25 do not exactly correspond to the actual strains **p**, **q** and **t**. The “misfit” vectors indicate the strain differences:

$$\mathbf{p}_{misfit} = \mathbf{p} - \frac{1+\nu}{E} \bar{\mathbf{a}} \mathbf{P} \quad (33)$$

$$\mathbf{q}_{misfit} = \mathbf{q} - \frac{1}{E} \bar{\mathbf{b}} \mathbf{Q} \quad (34)$$

$$\mathbf{t}_{misfit} = \mathbf{t} - \frac{1}{E} \bar{\mathbf{b}} \mathbf{T} \quad (35)$$

10.3.7 Calculate the mean squares of the misfit vectors:

$$p_{rms}^2 = \frac{1}{n} \sum_{j=1}^n (p_{misfit})_j^2 \quad (36)$$

$$q_{rms}^2 = \frac{1}{n} \sum_{j=1}^n (q_{misfit})_j^2 \quad (37)$$

$$t_{rms}^2 = \frac{1}{n} \sum_{j=1}^n (t_{misfit})_j^2 \quad (38)$$

10.3.8 If the values of  $p_{rms}^2$ ,  $q_{rms}^2$  and  $t_{rms}^2$  are within 5 % of the values of  $p_{std}^2$ ,  $q_{std}^2$  and  $t_{std}^2$  in Eq 20-22, accept the calculated values of **P**, **Q** and **T**. If not, make new guesses of the regularization factors:

$$(\alpha_P)_{new} = \frac{p_{std}^2}{p_{rms}^2} (\alpha_P)_{old} \quad (39)$$

$$(\alpha_Q)_{new} = \frac{q_{std}^2}{q_{rms}^2} (\alpha_Q)_{old} \quad (40)$$

$$(\alpha_T)_{new} = \frac{t_{std}^2}{t_{rms}^2} (\alpha_T)_{old} \quad (41)$$

10.3.9 Recalculate Eq 30-41 until the 5 % criterion is obeyed. Then accept the final values of **P**, **Q** and **T**.

10.3.10 Compute the Cartesian stresses:

$$(\sigma_x)_j = P_j - Q_j \quad (42)$$

$$(\sigma_y)_j = P_j + Q_j \quad (43)$$

$$(\tau_{xy})_j = T_j \quad (44)$$

10.3.11 Compute the principal stresses and direction:

$$(\sigma_{max})_k, (\sigma_{min})_k = P_k \pm \sqrt{Q_k^2 + T_k^2} \quad (45)$$

$$\beta_k = \frac{1}{2} \arctan\left(\frac{-T_k}{-Q_k}\right) \quad (46)$$

10.3.12 Place the angle  $\beta$  in the correct quadrant using the two-argument arctan function (function atan2 in some computer languages). Alternatively, the result from the one-argument calculation can be adjusted by  $\pm 90^\circ$  as necessary to place  $\beta$  within the appropriate range defined in Table 4.

10.3.13 A positive value of  $\beta$ , say  $\beta = 30^\circ$ , indicates that  $\sigma_{max}$  lies  $30^\circ$  clockwise of the direction of gage 1. A negative

value of  $\beta$ , say  $\beta = -30^\circ$ , indicates that  $\sigma_{max}$  lies  $30^\circ$  counter-clockwise of the direction of gage 1.

10.3.14 In general, the direction of  $\sigma_{max}$  will closely coincide with the direction of the numerically most negative (compressive) relieved strain. The case where both  $Q = 0$  and  $T = 0$  corresponds to an isotropic stress field, for which the angle  $\beta$  has no meaning.

10.3.15 Plot graphs of  $\sigma_{max}$  and  $\sigma_{min}$  versus hole depth. If several computed stresses significantly exceed 60 % of the material yield stress, then the results are not quantitative, and must be reported as “indicative” only. In general, the computed stresses whose values exceed 60 % of the material yield stress tend to be overestimated. Their actual values are usually smaller than indicated.

## 11. Report

### 11.1 Test Description:

11.1.1 Description of the test workpiece,

11.1.2 Material,

11.1.3 Pertinent mechanical properties,

11.1.4 Location of strain gage rosettes,

11.1.5 Model and type of rosettes used,

11.1.6 Rosette geometry, and

11.1.7 The method used to drill the hole.

### 11.2 “Thin” Workpiece with Uniform Stress:

11.2.1 Strain readings for each rosette, and

11.2.2 Calculated xy- and principal stresses at each rosette.

### 11.3 “Thick” Workpiece with Uniform Stress:

11.3.1 Plot of strain versus depth for each rosette,

11.3.2 Tabulation of strains  $\epsilon_1$ ,  $\epsilon_2$ , and  $\epsilon_3$  for each rosette, and

11.3.3 Calculated xy- and principal stresses at each rosette.

### 11.4 “Thick” Workpiece with Non-Uniform Stress:

11.4.1 Plot of strain versus depth for each rosette,

11.4.2 Tabulation of strains  $\epsilon_1$ ,  $\epsilon_2$ , and  $\epsilon_3$  for each rosette,

11.4.3 Estimate of standard strain errors for each rosette,

11.4.4 Tabulation and plot of calculated xy-stresses versus depth at each rosette, and

11.4.5 Tabulation of principal stresses and principal directions at each rosette.

## 12. Precision and Bias

### 12.1 Experimental Technique:

12.1.1 Operator skill and expertise are probably among the most important factors on the precision of the result. References (10) and (11) provide substantial practical guidance about how to make high-quality hole-drilling residual stress measurements. These publications are excellent preparatory reading, particularly for practitioners who infrequently make hole-drilling measurements.





TABLE 6

Table 6(a) Hole-Drilling Calibration Matrix  $\bar{a}$  for a  $\frac{1}{16}$  in. Type B Rosette with a 0.080 in. (2 mm) Hole

Hole Depth		Stress Depth									
		0.002	0.004	0.006	0.008	0.010	0.012	0.014	0.016	0.018	0.020 in.
in.	mm	0.05	0.10	0.15	0.20	0.25	0.30	0.35	0.40	0.45	0.50 mm
0.002	0.05	-0.00726									
0.004	0.10	-0.00878	-0.00766								
0.006	0.15	-0.01013	-0.00909	-0.00788							
0.008	0.20	-0.01133	-0.01037	-0.00924	-0.00793						
0.010	0.25	-0.01237	-0.01149	-0.01043	-0.00921	-0.00781					
0.012	0.30	-0.01325	-0.01245	-0.01147	-0.01033	-0.00901	-0.00751				
0.014	0.35	-0.01397	-0.01325	-0.01235	-0.01129	-0.01004	-0.00863	-0.00704			
0.016	0.40	-0.01471	-0.01388	-0.01297	-0.01214	-0.01088	-0.00956	-0.00811	-0.00654		
0.018	0.45	-0.01533	-0.01450	-0.01360	-0.01268	-0.01161	-0.01039	-0.00904	-0.00758	-0.00599	
0.020	0.50	-0.01587	-0.01504	-0.01414	-0.01313	-0.01217	-0.01105	-0.00981	-0.00845	-0.00696	-0.00536
0.022	0.55	-0.01634	-0.01550	-0.01460	-0.01367	-0.01257	-0.01147	-0.01046	-0.00909	-0.00774	-0.00633
0.024	0.60	-0.01672	-0.01589	-0.01500	-0.01406	-0.01299	-0.01190	-0.01082	-0.00964	-0.00839	-0.00708
0.026	0.65	-0.01705	-0.01621	-0.01532	-0.01441	-0.01332	-0.01225	-0.01118	-0.00997	-0.00892	-0.00764
0.028	0.70	-0.01735	-0.01651	-0.01561	-0.01468	-0.01362	-0.01255	-0.01148	-0.01031	-0.00921	-0.00810
0.030	0.75	-0.01759	-0.01675	-0.01586	-0.01493	-0.01387	-0.01280	-0.01174	-0.01059	-0.00945	-0.00840
0.032	0.80	-0.01781	-0.01697	-0.01607	-0.01515	-0.01408	-0.01302	-0.01196	-0.01080	-0.00974	-0.00860
0.034	0.85	-0.01799	-0.01715	-0.01625	-0.01533	-0.01426	-0.01320	-0.01213	-0.01099	-0.00992	-0.00881
0.036	0.90	-0.01814	-0.01730	-0.01640	-0.01550	-0.01441	-0.01334	-0.01229	-0.01114	-0.01008	-0.00897
0.038	0.95	-0.01829	-0.01744	-0.01654	-0.01561	-0.01454	-0.01347	-0.01242	-0.01129	-0.01021	-0.00912
0.040	1.00	-0.01843	-0.01757	-0.01666	-0.01573	-0.01465	-0.01358	-0.01253	-0.01140	-0.01035	-0.00925

Hole Depth		Stress Depth									
		0.022	0.024	0.026	0.028	0.030	0.032	0.034	0.036	0.038	0.040 in.
in.	mm	0.55	0.60	0.65	0.70	0.75	0.80	0.85	0.90	0.95	1.00 mm
0.022	0.55	-0.00486									
0.024	0.60	-0.00572	-0.00430								
0.026	0.65	-0.00637	-0.00509	-0.00379							
0.028	0.70	-0.00691	-0.00571	-0.00450	-0.00327						
0.030	0.75	-0.00730	-0.00619	-0.00506	-0.00392	-0.00277					
0.032	0.80	-0.00753	-0.00655	-0.00549	-0.00443	-0.00339	-0.00234				
0.034	0.85	-0.00775	-0.00674	-0.00581	-0.00484	-0.00387	-0.00291	-0.00195			
0.036	0.90	-0.00793	-0.00695	-0.00598	-0.00514	-0.00423	-0.00333	-0.00246	-0.00162		
0.038	0.95	-0.00809	-0.00710	-0.00617	-0.00528	-0.00449	-0.00366	-0.00285	-0.00207	-0.00131	
0.040	1.00	-0.00822	-0.00724	-0.00632	-0.00541	-0.00466	-0.00389	-0.00314	-0.00242	-0.00172	-0.00104

Table 6(b) Hole-Drilling Calibration Matrix  $\bar{b}$  for a  $\frac{1}{16}$  in. Type B Rosette with a 0.080 in. (2 mm) Hole

Hole Depth		Stress Depth									
		0.002	0.004	0.006	0.008	0.010	0.012	0.014	0.016	0.018	0.020 in.
in.	mm	0.05	0.10	0.15	0.20	0.25	0.30	0.35	0.40	0.45	0.50 mm
0.002	0.05	-0.01417									
0.004	0.10	-0.01653	-0.01516								
0.006	0.15	-0.01866	-0.01746	-0.01585							
0.008	0.20	-0.02055	-0.01953	-0.01810	-0.01624						
0.010	0.25	-0.02222	-0.02138	-0.02012	-0.01844	-0.01634					
0.012	0.30	-0.02365	-0.02299	-0.02190	-0.02040	-0.01848	-0.01614				
0.014	0.35	-0.02485	-0.02437	-0.02346	-0.02214	-0.02039	-0.01823	-0.01564			
0.016	0.40	-0.02610	-0.02547	-0.02459	-0.02375	-0.02195	-0.01997	-0.01769	-0.01510		
0.018	0.45	-0.02715	-0.02656	-0.02571	-0.02479	-0.02331	-0.02154	-0.01947	-0.01709	-0.01440	
0.020	0.50	-0.02806	-0.02750	-0.02670	-0.02561	-0.02440	-0.02283	-0.02097	-0.01879	-0.01631	-0.01353
0.022	0.55	-0.02888	-0.02833	-0.02755	-0.02664	-0.02517	-0.02365	-0.02225	-0.02008	-0.01787	-0.01546
0.024	0.60	-0.02958	-0.02906	-0.02830	-0.02740	-0.02598	-0.02450	-0.02298	-0.02119	-0.01919	-0.01699
0.026	0.65	-0.03019	-0.02968	-0.02894	-0.02808	-0.02666	-0.02521	-0.02370	-0.02186	-0.02030	-0.01816
0.028	0.70	-0.03072	-0.03023	-0.02950	-0.02864	-0.02727	-0.02584	-0.02435	-0.02257	-0.02089	-0.01910
0.030	0.75	-0.03116	-0.03068	-0.02998	-0.02914	-0.02778	-0.02638	-0.02491	-0.02316	-0.02139	-0.01976
0.032	0.80	-0.03158	-0.03108	-0.03038	-0.02956	-0.02822	-0.02684	-0.02539	-0.02366	-0.02202	-0.02022
0.034	0.85	-0.03192	-0.03143	-0.03073	-0.02990	-0.02859	-0.02723	-0.02580	-0.02410	-0.02247	-0.02071
0.036	0.90	-0.03221	-0.03173	-0.03104	-0.03022	-0.02891	-0.02756	-0.02616	-0.02444	-0.02287	-0.02112
0.038	0.95	-0.03247	-0.03200	-0.03131	-0.03048	-0.02919	-0.02785	-0.02645	-0.02475	-0.02317	-0.02146
0.040	1.00	-0.03268	-0.03222	-0.03154	-0.03074	-0.02944	-0.02810	-0.02671	-0.02501	-0.02342	-0.02173

Hole Depth		Stress Depth									
		0.022	0.024	0.026	0.028	0.030	0.032	0.034	0.036	0.038	0.040 in.
in.	mm	0.55	0.60	0.65	0.70	0.75	0.80	0.85	0.90	0.95	1.00 mm
0.022	0.22	-0.01285									
0.024	0.24	-0.01460	-0.01202								
0.026	0.26	-0.01596	-0.01367	-0.01126							
0.028	0.28	-0.01710	-0.01499	-0.01278	-0.01046						
0.030	0.30	-0.01795	-0.01603	-0.01401	-0.01188	-0.00964					

**TABLE 6** *Continued*

0.032	0.32	-0.01846	-0.01685	-0.01493	-0.01299	-0.01100	-0.00895				
0.034	0.34	-0.01899	-0.01729	-0.01567	-0.01390	-0.01207	-0.01019	-0.00825			
0.036	0.36	-0.01942	-0.01779	-0.01608	-0.01459	-0.01288	-0.01115	-0.00940	-0.00762		
0.038	0.38	-0.01979	-0.01817	-0.01650	-0.01493	-0.01349	-0.01191	-0.01030	-0.00866	-0.00700	
0.040	0.40	-0.02008	-0.01848	-0.01684	-0.01521	-0.01389	-0.01245	-0.01098	-0.00948	-0.00796	-0.00641

12.1.2 A Code of Practice for determining the uncertainties associated with the hole drilling technique has been produced as part of the UNCERT project (26).

12.1.3 Although there are no recognized residual stress reference materials, users are recommended to verify their measurements on components such as a beam in 4 point bending or a “ring and plug” component, with known stress distributions. Where possible, the hole drilling measurements should be validated with other techniques, and users are recommended to develop an uncertainty analysis for their set up both to identify and quantify the uncertainties contributing to the precision of their measurement.

12.1.4 Smaller sized rosettes offer the potential for measuring close to the surface. However, the experimentally generated errors associated with the measurements from such rosettes (accuracy of hole drilling, control of depth etc.) are likely to be higher than the corresponding measurements with larger rosettes.

#### 12.2 Uniform Stress Measurements:

12.2.1 Uniform residual stresses determined by the hole-drilling method may be expected to exhibit a bias not exceeding  $\pm 10\%$  provided that the residual stresses are actually uniform within the hole depth, and that the drilling technique does not induce significant machining stresses in the material (5, 23). The requirement that the residual stresses not vary significantly with depth is difficult to recognize with certainty because the stress uniformity test in Fig. 6 is not very sensitive (17). Residual stresses are commonly induced by various working, forming, welding, and other manufacturing processes that involve the application of energy to and through the surface of the object. Consequently, there are usually stress gradients near the surface, while uniform residual stresses are encountered only rarely. If a significant non-uniform stress distribution goes unrecognized, the error may be much more than 10 %, and will usually be in the direction of underestimating the maximum stress.

12.2.2 A round-robin test program (15) was carried out on AISI 1018 carbon-steel specimens that had been subjected to a prior stress relief treatment. High-speed (using an air turbine), low-speed (using a conventional drill), and air abrasive drilling were used. In all, 26 measurements were made by eight laboratories on eight nominally identical specimens, giving a standard deviation of 2.0 ksi (14 MPa) among the measurements.

12.2.3 A round-robin test program (24) was carried out on type 304 stainless steel specimens that had been subjected to a prior stress relief treatment. In all, 46 nominally identical specimens were tested by 35 laboratories using a variety of methods. Forty-six residual stress measurements, made using high-speed drilling and air abrasive drilling, produced standard

deviations that did not exceed 1.7 ksi (12 MPa). Results of six measurements made using low-speed drilling were not consistent.

12.2.4 The variability of results obtained on stressed specimens may be expected to be considerably greater than that observed with relatively stress-free specimens. A round-robin test program on stressed stainless steel specimens is being planned by the Residual Stress Technical Division of the Society for Experimental Mechanics with participation by ASTM Subcommittee E28.13.

12.2.5 Evaluations of the precision of the hole-drilling method as applied to carbon or stainless steels may not be applicable to other materials, which exhibit machineability characteristics that differ considerably from those of steel and even from each other. The high-speed hole drilling technique has been reported as being effective with such diverse materials as copper, aluminum, zirconium and stellite (14).

12.2.6 Random experimental errors occur at individual drilling depths from events like strain reading errors, strain gage anomalies, and test environment changes. The use of Eq 15-17 reduces the influence of random experimental errors on the residual stress results, and improves the precision (19).

12.2.7 Use of the six-element type C rosette increases electrical output for a given residual stress level, compared with the three-element types A and B. This increase in electrical sensitivity can improve the precision of the hole-drilling measurements (19). However, use of six-element rosettes involves greater installation effort and expense. For general-purpose work, rosette types A and B typically give satisfactory results. Type C rosettes are appropriate for critical applications and for work with thermal low-conductivity materials.

#### 12.3 Non-Uniform Stress Measurements:

12.3.1 An extensive program to evaluate non-uniform stress measurement accuracy has not yet been carried out, but standard deviations are expected to be much larger than for uniform stress measurements. Some studies have examined the application of the hole drilling method to non-uniform stress fields generated by shot peening (25). Because of the steepness of the stress gradient, a single value for uncertainty or standard deviation cannot be identified. The stress values measured must be compared over a range of depths. The results generally showed larger variations than observed with uniform stress fields, particularly in the steps closest to the surface.

12.3.2 Some of the factors controlling the precision and accuracy of the results include: drill misalignment, the presence of large strain gradients near the surface, the smaller gauge outputs in the first few drilling steps and identification of the zero reference surface.



TABLE 7

Table 7(a) Hole-Drilling Calibration Matrix  $\bar{a}$  for a  $\frac{1}{16}$  in. Type C Rosette with a 0.080 in. (2 mm) Hole

		Stress Depth									
Hole Depth in.	mm	0.002 0.05	0.004 0.10	0.006 0.15	0.008 0.20	0.010 0.25	0.012 0.30	0.014 0.35	0.016 0.40	0.018 0.45	0.020 in. 0.50 mm
0.002	0.05	-0.01704									
0.004	0.10	-0.02009	-0.01741								
0.006	0.15	-0.02285	-0.02043	-0.01749							
0.008	0.20	-0.02531	-0.02315	-0.02047	-0.01730						
0.010	0.25	-0.02748	-0.02557	-0.02316	-0.02024	-0.01681					
0.012	0.30	-0.02945	-0.02757	-0.02547	-0.02310	-0.01965	-0.01608				
0.014	0.35	-0.03124	-0.02938	-0.02730	-0.02526	-0.02212	-0.01885	-0.01523			
0.016	0.40	-0.03282	-0.03092	-0.02886	-0.02668	-0.02402	-0.02133	-0.01775	-0.01417		
0.018	0.45	-0.03422	-0.03230	-0.03023	-0.02806	-0.02549	-0.02306	-0.01988	-0.01659	-0.01307	
0.020	0.50	-0.03545	-0.03347	-0.03137	-0.02921	-0.02669	-0.02422	-0.02148	-0.01867	-0.01521	-0.01192
0.022	0.55	-0.03649	-0.03451	-0.03241	-0.03020	-0.02774	-0.02530	-0.02269	-0.02012	-0.01695	-0.01386
0.024	0.60	-0.03735	-0.03534	-0.03324	-0.03108	-0.02865	-0.02621	-0.02370	-0.02123	-0.01824	-0.01546
0.026	0.65	-0.03810	-0.03609	-0.03399	-0.03178	-0.02942	-0.02700	-0.02448	-0.02212	-0.01926	-0.01661
0.028	0.70	-0.03872	-0.03672	-0.03461	-0.03241	-0.03006	-0.02771	-0.02510	-0.02268	-0.02005	-0.01753
0.030	0.75	-0.03927	-0.03727	-0.03516	-0.03293	-0.03059	-0.02826	-0.02568	-0.02320	-0.02064	-0.01823
0.032	0.80	-0.03972	-0.03772	-0.03563	-0.03343	-0.03101	-0.02869	-0.02615	-0.02371	-0.02117	-0.01877
0.034	0.85	-0.04014	-0.03811	-0.03600	-0.03382	-0.03141	-0.02905	-0.02654	-0.02411	-0.02161	-0.01924
0.036	0.90	-0.04050	-0.03845	-0.03632	-0.03412	-0.03173	-0.02935	-0.02688	-0.02445	-0.02198	-0.01964
0.038	0.95	-0.04083	-0.03874	-0.03658	-0.03436	-0.03199	-0.02960	-0.02712	-0.02477	-0.02230	-0.01996
0.040	1.00	-0.04110	-0.03899	-0.03682	-0.03458	-0.03223	-0.02983	-0.02735	-0.02497	-0.02256	-0.02024
0.042	1.05	-0.04131	-0.03920	-0.03702	-0.03477	-0.03244	-0.03010	-0.02756	-0.02513	-0.02274	-0.02048
0.044	1.10	-0.04149	-0.03938	-0.03720	-0.03493	-0.03262	-0.03028	-0.02775	-0.02531	-0.02290	-0.02064
0.046	1.15	-0.04162	-0.03952	-0.03734	-0.03509	-0.03275	-0.03043	-0.02790	-0.02548	-0.02306	-0.02077
0.048	1.20	-0.04175	-0.03965	-0.03748	-0.03521	-0.03287	-0.03054	-0.02802	-0.02561	-0.02320	-0.02091
0.050	1.25	-0.04188	-0.03977	-0.03759	-0.03535	-0.03298	-0.03061	-0.02811	-0.02572	-0.02330	-0.02103

		Stress Depth									
Hole Depth in.	mm	0.022 0.55	0.024 0.60	0.026 0.65	0.028 0.70	0.030 0.75	0.032 0.80	0.034 0.85	0.036 0.90	0.038 0.95	0.040 in. 1.00 mm
0.022	0.55	-0.01074									
0.024	0.60	-0.01243	-0.00949								
0.026	0.65	-0.01385	-0.01110	-0.00835							
0.028	0.70	-0.01492	-0.01248	-0.00983	-0.00728						
0.030	0.75	-0.01572	-0.01344	-0.01102	-0.00864	-0.00630					
0.032	0.80	-0.01633	-0.01408	-0.01185	-0.00978	-0.00753	-0.00540				
0.034	0.85	-0.01682	-0.01461	-0.01246	-0.01052	-0.00851	-0.00653	-0.00456			
0.036	0.90	-0.01724	-0.01501	-0.01296	-0.01100	-0.00924	-0.00742	-0.00561	-0.00381		
0.038	0.95	-0.01756	-0.01540	-0.01334	-0.01142	-0.00968	-0.00810	-0.00639	-0.00476	-0.00317	
0.040	1.00	-0.01785	-0.01567	-0.01366	-0.01175	-0.01008	-0.00849	-0.00699	-0.00547	-0.00401	-0.00259
0.042	1.05	-0.01808	-0.01589	-0.01388	-0.01204	-0.01037	-0.00883	-0.00733	-0.00596	-0.00468	-0.00335
0.044	1.10	-0.01828	-0.01609	-0.01410	-0.01224	-0.01062	-0.00909	-0.00765	-0.00631	-0.00511	-0.00392
0.046	1.15	-0.01843	-0.01631	-0.01429	-0.01242	-0.01081	-0.00932	-0.00788	-0.00658	-0.00541	-0.00434
0.048	1.20	-0.01855	-0.01643	-0.01444	-0.01258	-0.01098	-0.00949	-0.00807	-0.00679	-0.00565	-0.00463
0.050	1.25	-0.01865	-0.01652	-0.01455	-0.01271	-0.01111	-0.00964	-0.00822	-0.00695	-0.00581	-0.00485

		Stress Depth				
Hole Depth in.	mm	0.042 1.05	0.044 1.10	0.046 1.15	0.048 1.20	0.050 in. 1.25
0.042	1.05	-0.00210				
0.044	1.10	-0.00278	-0.00168			
0.046	1.15	-0.00331	-0.00230	-0.00137		
0.048	1.20	-0.00367	-0.00275	-0.00188	-0.00105	
0.050	1.25	-0.00393	-0.00304	-0.00227	-0.00151	-0.00076

Table 7(b) Hole-Drilling Calibration Matrix  $\bar{b}$  for a  $\frac{1}{16}$  in. Type C Rosette with a 0.080 in. (2 mm) Hole

		Stress Depth									
Hole Depth in.	mm	0.002 0.05	0.004 0.10	0.006 0.15	0.008 0.20	0.010 0.25	0.012 0.30	0.014 0.35	0.016 0.40	0.018 0.45	0.020 in. 0.50 mm
0.002	0.05	-0.02533									
0.004	0.10	-0.02958	-0.02675								
0.006	0.15	-0.03345	-0.03109	-0.02767							
0.008	0.20	-0.03693	-0.03504	-0.03209	-0.02808						
0.010	0.25	-0.04004	-0.03862	-0.03614	-0.03259	-0.02798					
0.012	0.30	-0.04292	-0.04164	-0.03970	-0.03704	-0.03244	-0.02744				
0.014	0.35	-0.04555	-0.04439	-0.04258	-0.04050	-0.03641	-0.03194	-0.02670			
0.016	0.40	-0.04790	-0.04676	-0.04511	-0.04293	-0.03961	-0.03607	-0.03095	-0.02563		
0.018	0.45	-0.05005	-0.04892	-0.04728	-0.04526	-0.04211	-0.03909	-0.03458	-0.02976	-0.02442	
0.020	0.50	-0.05200	-0.05084	-0.04918	-0.04711	-0.04419	-0.04115	-0.0373	-0.03340	-0.02817	-0.02304

**TABLE 7** *Continued*

0.022	0.55	-0.05363	-0.05253	-0.05092	-0.04881	-0.04599	-0.04307	-0.03955	-0.03601	-0.03129	-0.02654
0.024	0.60	-0.05495	-0.05391	-0.05237	-0.05036	-0.04758	-0.04467	-0.04136	-0.03798	-0.03362	-0.02952
0.026	0.65	-0.05614	-0.05513	-0.05362	-0.05164	-0.04893	-0.04609	-0.04280	-0.03962	-0.03548	-0.03163
0.028	0.70	-0.05714	-0.05615	-0.05469	-0.05276	-0.05007	-0.04730	-0.04397	-0.04076	-0.03696	-0.03326
0.030	0.75	-0.05804	-0.05706	-0.05560	-0.05371	-0.05105	-0.04829	-0.04503	-0.04179	-0.03811	-0.03461
0.032	0.80	-0.05882	-0.05782	-0.05635	-0.05448	-0.05186	-0.04915	-0.04590	-0.04273	-0.03912	-0.03565
0.034	0.85	-0.05949	-0.05850	-0.05704	-0.05514	-0.05255	-0.04985	-0.04664	-0.04350	-0.03996	-0.03657
0.036	0.90	-0.06006	-0.05908	-0.05762	-0.05571	-0.05315	-0.05044	-0.04727	-0.04412	-0.04068	-0.03734
0.038	0.95	-0.06051	-0.05955	-0.05811	-0.05622	-0.05364	-0.05100	-0.04781	-0.04465	-0.04125	-0.03799
0.040	1.00	-0.06091	-0.05997	-0.05854	-0.05664	-0.05407	-0.05142	-0.04828	-0.04513	-0.04176	-0.03850
0.042	1.05	-0.06124	-0.06030	-0.05888	-0.05703	-0.05444	-0.05175	-0.04865	-0.04559	-0.04218	-0.03895
0.044	1.10	-0.06153	-0.06059	-0.05918	-0.05733	-0.05478	-0.05208	-0.04898	-0.04592	-0.04254	-0.03932
0.046	1.15	-0.06175	-0.06083	-0.05943	-0.05757	-0.05505	-0.05243	-0.04927	-0.04618	-0.04282	-0.03962
0.048	1.20	-0.06195	-0.06104	-0.05965	-0.05779	-0.05528	-0.05267	-0.04953	-0.04644	-0.04308	-0.03986
0.050	1.25	-0.06211	-0.06122	-0.05984	-0.05801	-0.05547	-0.05285	-0.04972	-0.04667	-0.04331	-0.04009

Stress Depth											
Hole Depth		0.022	0.024	0.026	0.028	0.030	0.032	0.034	0.036	0.038	0.040 in.
in.	mm	0.55	0.60	0.65	0.70	0.75	0.80	0.85	0.90	0.95	1.00 mm
0.022	0.55	-0.02155									
0.024	0.60	-0.02466	-0.01984								
0.026	0.65	-0.02733	-0.02289	-0.01827							
0.028	0.70	-0.02935	-0.02559	-0.02113	-0.01677						
0.030	0.75	-0.03085	-0.02745	-0.02345	-0.01944	-0.01536					
0.032	0.80	-0.03202	-0.02862	-0.02506	-0.02168	-0.01784	-0.01406				
0.034	0.85	-0.03300	-0.02966	-0.02624	-0.02314	-0.1978	-0.01633	-0.01275			
0.036	0.90	-0.03382	-0.03048	-0.02723	-0.02407	-0.02126	-0.01813	-0.01487	-0.01149		
0.038	0.95	-0.03448	-0.03124	-0.02799	-0.02494	-0.02211	-0.01956	-0.01647	-0.01341	-0.01034	
0.040	1.00	-0.03505	-0.03182	-0.02864	-0.02561	-0.02290	-0.02031	-0.01771	-0.01495	-0.01216	-0.00935
0.042	1.05	-0.03550	-0.03229	-0.02915	-0.02620	-0.02348	-0.02095	-0.01842	-0.01600	-0.01363	-0.01102
0.044	1.10	-0.03590	-0.03269	-0.02961	-0.02666	-0.02400	-0.02146	-0.01908	-0.01675	-0.01459	-0.01227
0.046	1.15	-0.03623	-0.03308	-0.02999	-0.02710	-0.02444	-0.02191	-0.01955	-0.01733	-0.01523	-0.01311
0.048	1.20	-0.03650	-0.03337	-0.03030	-0.02743	-0.02480	-0.02229	-0.01996	-0.01776	-0.01576	-0.01373
0.050	1.25	-0.03674	-0.03361	-0.03055	-0.02770	-0.02507	-0.02263	-0.02028	-0.01810	-0.01609	-0.01420

Stress Depth						
Hole Depth		0.042	0.044	0.046	0.048	0.050 in.
in.	mm	1.05	1.10	1.15	1.20	1.25
0.042	1.05	-0.00854				
0.044	1.10	-0.01000	-0.00775			
0.046	1.15	-0.01116	-0.00907	-0.00703		
0.048	1.20	-0.01191	-0.01010	-0.00824	-0.00637	
0.050	1.25	-0.01241	-0.01081	-0.00926	-0.00751	-0.00582

12.3.3 Identification of the reference surface is particularly important with near-surface measurements because the uncertainties in defining this position can strongly influence the calculation of stress in the first increment. In such cases, the uncertainty in defining this position can be of the same order as the surface roughness.

### 13. Keywords

13.1 hole-drilling; integral method; residual stress measurement; strain gages; stress analysis

### REFERENCES

- (1) Rendler, N. J., and Vigness, I., "Hole-Drilling Strain Gage Method of Measuring Residual Stresses," *Experimental Mechanics*, Vol 6, No. 12, 1966, pp. 577–586.
- (2) Lu, J. (ed.), "Handbook of Measurement of Residual Stresses," *Society for Experimental Mechanics*, Fairmont Press, Lilburn, GA, 1996, Chapter 2.
- (3) Schajer, G. S., "Application of Finite Element Calculations to Residual Stress Measurements," *Journal of Engineering Materials and Technology*, *Transactions*, ASME, Vol 103, April 1981, pp. 157–163.
- (4) Schajer, G. S. "Measurement of Non-Uniform Residual Stresses Using the Hole Drilling Method," *Journal of Engineering Materials and Technology*, Vol 110, No. 4, 1988, Part I: pp. 338–343, Part II: pp. 344–349.
- (5) Beaney, E. M., "Accurate Measurements of Residual Stress on Any Steel Using the Centre Hole Method," *Strain*, *Journal BSSM*, Vol 12, No. 3, 1976, pp. 99–106.
- (6) Beghini, M., Bertini, L., and Raffaelli, P. "An Account of Plasticity in the Hole-Drilling Method of Residual Stress Measurement," *Journal of Strain Analysis*, Vol 30, No. 3, 1995.
- (7) Perry, C. G. "Data-Reduction Algorithms for Strain-Gage Rosette Measurements," *Experimental Techniques*, Vol 12, No. 5, 1989, pp. 13–18.
- (8) Schajer, G. S., and Tootoonian, M., "A New Rosette Design for More Reliable Hole-Drilling Residual Stress Measurements," *Experimental Mechanics*, Vol 37, No. 3, 1997, pp. 299–306.
- (9) Perry, C. C., and Lissner, H. R., *Strain Gage Primer*, McGraw-Hill





- Book Co., Inc., New York, NY, 1955.
- (10) “Measurement of Residual Stresses by the Hole Drilling Strain Gage Method,” *Tech Note TN-503-6*, Vishay Measurements Group, Raleigh, NC, 1996.
  - (11) Grant, P. V., Lord, J. D., and Whitehead P. S., “The Measurement of Residual Stresses by the Incremental Hole Drilling Technique,” *Measurement Good Practice Guide No. 53*, National Physical Laboratory, UK, 2002.
  - (12) Owens, A., “In-situ Stress Determination used in Structural Assessment of Concrete Structures,” *Strain*, Vol 29, 1993, pp. 115–123.
  - (13) Flaman, M. T., “Investigation of Ultra-High Speed Drilling for Residual Stress Measurements by the Center Hole Method,” *Experimental Mechanics*, Vol 22, No. 1, 1982, pp. 26–30.
  - (14) Flaman, M. T., and Herring, J. A., “Comparison of Four Hole-Producing Techniques for the Center-Hole Residual-Stress Measurement Method,” *Experimental Techniques*, Vol 9, No. 8, 1985, pp. 30–32.
  - (15) Yavelak, J. J. (compiler), “Bulk-Zero Stress Standard—AISI 1018 Carbon-Steel Specimens, Round Robin Phase 1,” *Experimental Techniques*, Vol 9, No. 4, 1985, pp. 38–41.
  - (16) Flaman, M. T., and Herring, J. A., “Ultra-High-Speed Center-Hole Technique for Difficult Machining Materials,” *Experimental Techniques*, Vol 10, No. 1, 1986, pp. 34–35.
  - (17) Schajer, G. S., “Judgment of Residual Stress Field Uniformity when Using the Hole-Drilling Method,” *Proceedings of the International Conference on Residual Stresses II*, Nancy, France. November 23–25, 1988, pp. 71–77.
  - (18) Schajer, G. S., “Strain Data Averaging for the Hole-Drilling Method,” *Experimental Techniques*, Vol 15, No. 2, 1991, pp. 25–28.
  - (19) Kroenke, W.C., Holloway, A.M., and Mabe, W.R., “Stress Calculation Update in ASTM E 837 Residual Stress Hole Drilling Standard”, *Advances in Computational Engineering & Sciences*, Tech Science Press, Vol 1, 2000, p. 695–699.
  - (20) Schajer, G. S., “Hole-Drilling Residual Stress Profiling with Automated Smoothing,” *Journal of Engineering Materials and Technology*, Vol 129, No. 3, 2007, pp. 440–445.
  - (21) Tikhonov, A., Goncharsky, A., Stepanov, V., and Yagola, A., “Numerical Methods for the Solution of Ill-Posed Problems,” Kluwer, Dordrecht, 1995.
  - (22) Tjhung, T., and Li, K., “Measurement of In-plane Residual Stresses Varying with Depth by the Interferometric Strain/Slope Rosette and Incremental Hole-Drilling,” *Journal of Engineering Materials and Technology*, Vol 125, No. 2, 2003, pp. 153–162.
  - (23) Beaney, E. M., and Procter, E., “A Critical Evaluation of the Centre Hole Technique for the Measurement of Residual Stresses,” *Strain*, Vol 10, No. 1, 1974, pp. 7–14, 52.
  - (24) Flaman, M. T., and Herring, J. A., “SEM/ASTM Round-Robin Residual-Stress-Measurement Study—Phase 1, 304 Stainless-Steel Specimen,” *Experimental Techniques*, Vol 10, No. 5, 1986, pp. 23–25.
  - (25) Lord, J. D., Grant, P. V., Fry, A. T., and Kandil, F. A., “A UK Residual Stress Intercomparison Exercise—Development of Measurement Good Practice for the XRD and Hole Drilling Techniques,” *ECRS-6*, Coimbra, Portugal, Materials Science Forum, Vols 404–407, 2002, pp. 567–572.
  - (26) Oettel, R., “The Determination of Uncertainties in Residual Stress Measurement (using the Hole Drilling Technique),” *Code of Practice*, No. 15, Issue 1, September 2000, EU Project No. SMT4-CT97-2165.

ASTM International takes no position respecting the validity of any patent rights asserted in connection with any item mentioned in this standard. Users of this standard are expressly advised that determination of the validity of any such patent rights, and the risk of infringement of such rights, are entirely their own responsibility.

This standard is subject to revision at any time by the responsible technical committee and must be reviewed every five years and if not revised, either reapproved or withdrawn. Your comments are invited either for revision of this standard or for additional standards and should be addressed to ASTM International Headquarters. Your comments will receive careful consideration at a meeting of the responsible technical committee, which you may attend. If you feel that your comments have not received a fair hearing you should make your views known to the ASTM Committee on Standards, at the address shown below.

This standard is copyrighted by ASTM International, 100 Barr Harbor Drive, PO Box C700, West Conshohocken, PA 19428-2959, United States. Individual reprints (single or multiple copies) of this standard may be obtained by contacting ASTM at the above address or at 610-832-9585 (phone), 610-832-9555 (fax), or service@astm.org (e-mail); or through the ASTM website (www.astm.org).